ANALYSIS OF MAGNETIC AMPLIFIER WITH CAPACITIVE LOADING

IN KU KANG

ANALYSIS OF MAGNETIC AMPLIFIER WITH CAPACITIVE LOADING

* * * *

Kang, In Ku

ANALYSIS OF MAGNETIC AMPLIFIER

WITH CAPACITIVE LOADING

by

Kang, In Ku
//
Lieutenant, Republic of Korea Navy

Submitted in partial fulfillment of
the requirements for the degree of

MASTER OF SCIENCE
IN
ELECTRICAL ENGINEERING

United States Naval Postgraduate School
Monterey, California

1 9 6 1

ANALYSIS OF MAGNETIC AMPLIFIER WITH CAPACITIVE LOADING

by

Kang, In Ku

This work is accepted as fulfilling

the thesis requirements for the degree of

MASTER OF SCIENCE

IN

ELECTRICAL ENGINEERING

from the

United States Naval Postgraduate School

ABSTRACT

The operation of a magnetic amplifier with capacitive loading is analytically and experimentally examined. The difference equation is used for analytical work and several essential approximations are made. The steady state load current equation is derived as a function of control voltage, which is in fair agreement with the experimental results. The maximum applicable voltage with capacitive loading is discussed and its equations are derived. The transient behaviour is found very complex, which is observed qualitatively.

Some peculiar phenomena are observed and their relations with circuit parameters are discussed. It is, however, felt that further investigation must be done to clarify some of the phenomena.

The writer wishes to express his appreciation for the assistance and encouragement given by Professor Charles H. Rothauge, without which this project may not be accomplished.

TABLE OF CONTENTS

LIST OF ILLUSTRATIONS

TABLE OF SYMBOLS AND ABBREVIATIONS

B_s	Maximum flux density (saturated)
e_1	Induced emf of core 1
e_2	Induced emf of core 2
E_c	The magnitude of control voltage
E_f	Forward constant voltage drop of a rectifier
E_g	Gate voltage, source voltage minus E_f
E_s	The magnitude of square wave source voltage or the peak value of sinusoidal source voltage.
E_{sr}	rms value of sinusoidal source voltage
E_s^*	Saturation voltage
H_m	Dynamic magnetizing force
I_m	Magnetizing current, $Im = \frac{H_m l}{N_g}$
I_L	Half cycle average load current
N	Turns ration, $N = N_g/N_c$
N_c	Number of turns of control winding
N_g	Number of turns of gate winding
φ	Phase angle, $\varphi = \tan^{-1}\frac{1}{\omega\tau}$
R_c	Total resistance of control circuit
R_g	Gate resistance
R_L	Load resistance
R_o	Total resistance of gate circuit
$\bar{S}$	Control parameter $\bar{S} = \frac{E_c}{NR_c I_m}$
T	Period of the source voltage
τ	Time constant of gate circuit, $\tau = R_o C$

t_s Time at which the core saturates

V Voltage drop across the capacitor

ω Angular velocity of the source voltage, $\omega = \frac{2\pi}{T}$

* Subscript n, n + 1 ---- Represent n, n + 1 ---- half cycle

* Subscript A, B, C, ---- Represent Mode A, B, C, ----

* Refer AIEE committee report [8]

1. Introduction.

The magnetic amplifier has been used successfully with resistive and inductive loading, and recently their usage has been extended to loads which should be described in terms of capacitance and resistance [3]. Even though there have been many analyses of magnetic amplifiers, few papers have dealt with capacitive loading. One recently published paper by Dr. Bourne and Dr. Salihi has extensively analysed the series connected saturable reactor with capacitive loading [1]. The operation of the magnetic amplifier is quite different from that of a series saturable reactor. This work examines analytically and experimentally the operation of a doubler type magnetic amplifier with capacitive loading.

The difference equation has been effectively used to anlayse a magnetic amplifier with resistive loading [6]. The same technique is adapted for use in this work. Although the difference equation is interpreted in terms of a transfer of the Ztransformation, an approximation to a differential equation may be used for slower response time.

Capacitive loading further complicates the already non-linear magnetic amplifier, so that approximation is inevitable if the operation is to be analysed. The experimental results, however, justify the approximation.

For the same reason, rectangular wave source voltage is applied, but the steady state characteristic with sinusoidal source voltage is also derived, showing the complexity of the equation.

2. The Circuit

The magnetic amplifier circuit that is analysed in the paper is the A-C doubler circuit of Fig. 1. This amplifier consists of two identical cores wound with identical gate windings and control windings.

The source voltage is a square wave voltage of which the internal impedance is negligible. The resistance of the gate winding is R_g in which the forward resistance of the rectifier can be included. R_L is the load resistance and R_c is the total resistance of control circuit including the resistances of two control windings.

The experimental circuit is slightly modified to enable the measurement of load current as shown in Fig. 2.

The sum of R_1 and R_2 is equal to R_L of Fig. 1, and R_1 is the resistance of ammeter.

The cores used in this experiment are a matched pair of 50106 (HYMU80, Magnetic INC Products) having gate windings of 1000 turns; each control winding of 500 turns.

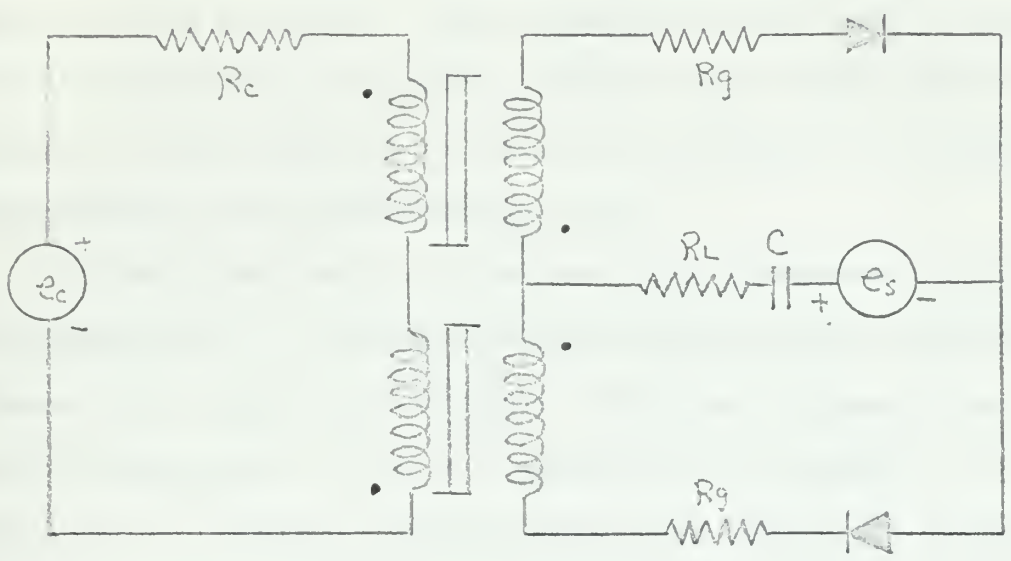

Fig. 1 AC Doubler Circuit (Analytical)

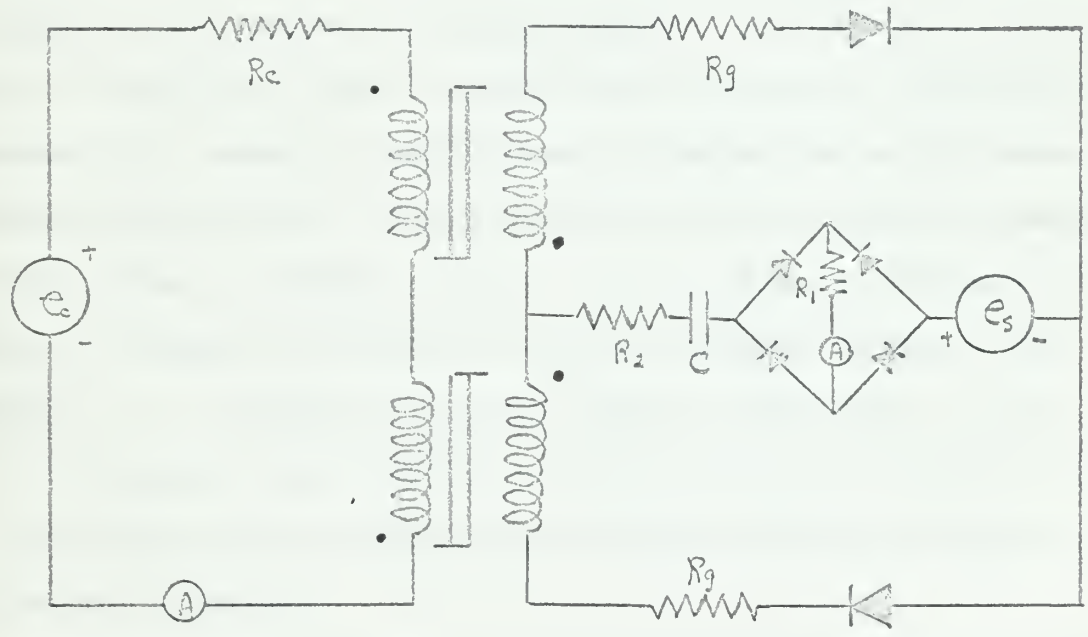

Fig. 2 AC Doubler Circuit(Experimental)

3. Assumptions

It is well known that the magnetization characteristic of the magnetic core is non-linear. Many approaches have been made to approximate this non-linearity and recently several complex expressions have been reported, but these failed to give accurate predictions of the operation characteristic of the magnetic amplifier [4].

Furthermore, application of those analytical expressions of magnetization characteristic in this analysis would result in such a complicated equation that it might not be solvable. Therefore, a dynamic magnetization characteristic of Fig. 3 is assumed for this analysis. B is flux density and H_m represents apparent magnetizing force which includes all magnetizing forces required to overcome eddy current effects as well as d-c coercive force of the core itself, and therefore H_m is a function of the magnitude and frequency of voltage applied. It is also assumed that when flux density of a core is changing due to the control voltage alone, the magnetizing current is negligible and no leakage flux exists between windings after saturation. The characteristic of the rectifier is assumed as shown in Fig. 4. Forward resistance, R_f is linear and backward resistance is assumed to be infinite within the operation voltage of this amplifier. E_f represents the forward constant voltage drop. As a result the equivalent circuit of the rectifier will be R_f in series with E_f which opposes source voltage in one direction and an open circuit in the backward direction.

All other circuit components are ideal, namely the winding capacitance of the reactor, the capacitance of rectifier, and the leakage resistance of the capacitor are negligible.

For the simplicity of the analysis a rectangular voltage source and d-c control voltage are assumed.

$$e_s = + E_s \quad o < t < t/2$$
$$\quad - E_s \quad t/2 < t < T \qquad (1)$$

$$e_c = - E_c$$

The sign of the control voltage with respect to the circuit diagram is negative, which will become evident in later discussion.

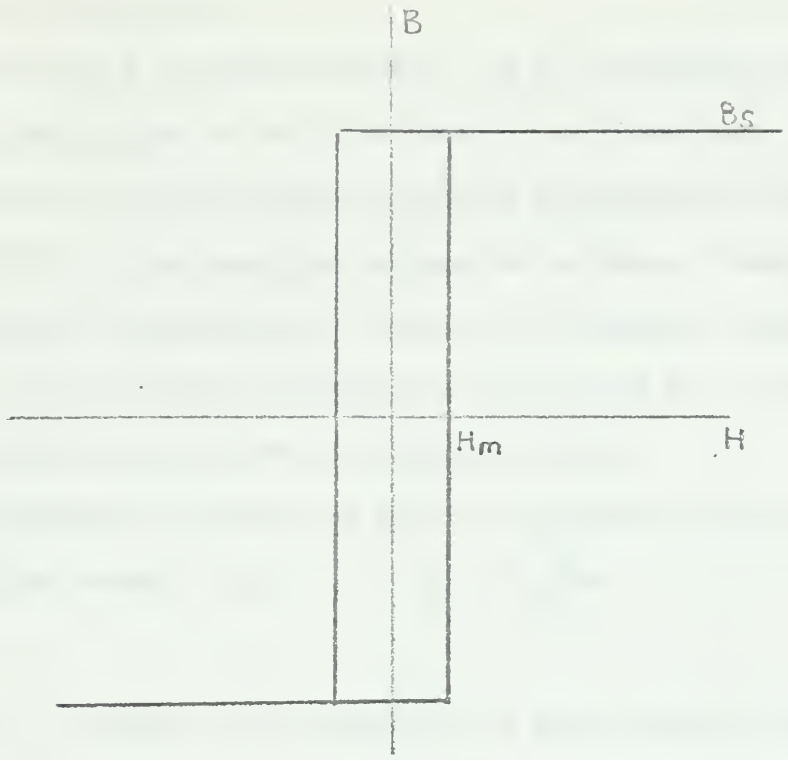

Fig. 3 Magnetization Characteristic Curve

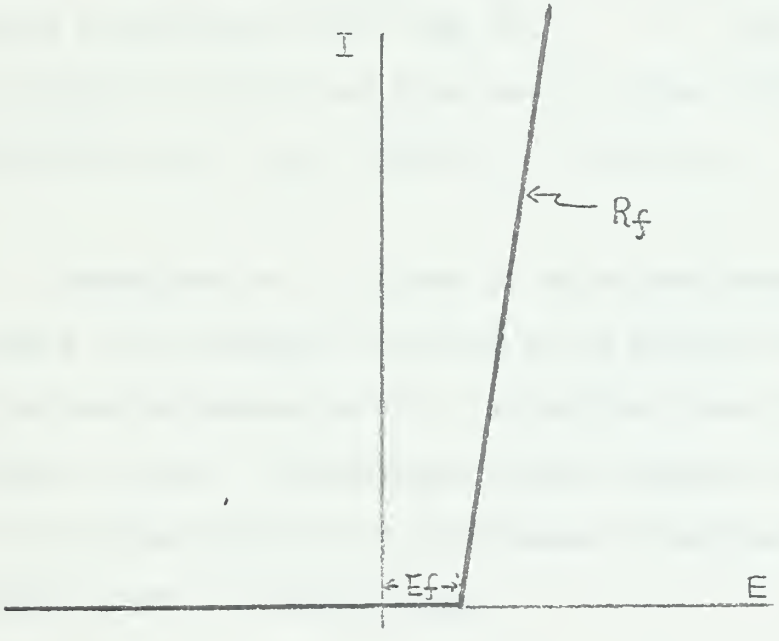

Fig. 4 Characteristic Curve of a Silicon Rectifier

4. Modes of Operations

In analysing a non-linear circuit, one of the effective ways is to divide it into regions in which the behavior is linearized. This method is very adequate for this analysis since it is assumed that magnetization characteristics of the cores are rectangular in shape. There are six possible modes, of which two are undesirable, depending on the state of each core. The appropriate equations are developed for each mode and boundary condition are matched to get the solution.

For convenience, magnetizing force is referred to the gate circuit as magnetizing current, I_m. $I_m = \frac{H_m l}{N_g}$

Also, R_o denotes total resistance of gate circuit in series, namely $R_o = R_g + R_L$. And the gate voltage, e_g is defined as equivalent voltage applied to the gate circuit, that is $e_g = e_s - e_f$.

The subscripts A, B, C, D, and E are used to assign the functions to corresponding modes, e. g. i_{LA} denotes i_L in mode A etc.

Mode A. Assume that at $t = 0$, core 1 is at some intermediate flux level and core 2 is at saturation. As soon as the positive voltage with respect to the polarity marking of Fig. 1 is applied, core 2 starts to reset and core 1 to gate. The equivalent circuit diagram is shown in Fig. 5a. The following equations may be obtained by applying Kirchhoffs' law and assuming equality of ampere-turns:

$$e_c = R_c i_C + \frac{e_1}{N} - \frac{e_2}{N}$$

$$e_g = -V_A + i_L R_o + e_1 + \frac{1}{C}\int i_L dt$$

$$i_L = \frac{i_C}{N} = I_m \qquad \text{for Core 1 gating}$$

$$\frac{i_C}{N} = -I_m . \qquad \text{for Core 2 resetting}$$

where e_1 and e_2 are induced emf's of core 1 and 2 respectively and referred to the gate winding. From these equations, e_1, e_2, and i_L in this mode are derived,

$$e_{1A} = e_g + V_A - 2I_m R_o - \frac{2}{C} I_m t_{SA} \tag{2}$$

$$e_{2A} = e_{1A} - Ne_C - N^2 R_c I_m \tag{3}$$

$$i_{LA} = 2I_m . \tag{4}$$

Mode B At $t = t_{sA}$, core 1 is saturated. Since the saturation region of the magnetization characteristic of the core is assumed to be horizontal, there is no flux linkage between the two windings of core 1 in this mode. The equivalent circuit diagram is shown in Fig. 5b and the following equations are obtained with the assumption that average magnetizing current in this mode is zero:

$$e_g = i_L R_o + \frac{1}{C}\int i_L dt - V_B \tag{5}$$

$$e_2 = -Ne_C . \tag{6}$$

This mode ends at the end of the half cycle, $t = \frac{T}{2}$.

Mode C In this mode, core 2 saturates negatively followed by the saturation of core 1. Since the controllable range of values of load current is decreased under these conditions, operation of the magnetic amplifier in this mode is not desirable. In case of resistive loading, the operation in this mode can be avoided very easily, but additional criteria is needed with capacitive loading which will be discussed in a later section. The equivalent circuit diagram is shown in Fig. 5c. Leakage flux between the two winding can not be neglected in this mode with practical cores. It should be pointed out that if this mode occurs, mode B will not occur and vice versa.

Mode D At $t = \frac{T}{2}$, the polarity of e_g will change to negative and core 1 starts to reset and core 2 to gate. The equivalent circuit diagram is shown in Fig. 5d.

Applying Kirchhoff's law and assuming equality of ampere turns, the following equations may be derived:

$$e_{2D} = e_g - V_c - 2I_m R_o - \frac{2}{C} I_m t_{SD} \qquad (7)$$

$$e_{1D} = e_{2D} + N e_c + N^2 R_c I_m \qquad (8)$$

$$i_{LD} = -2I_m .$$

Mode E At $t = \frac{T}{2} + t_{SD}$, core 2 is saturated. The equivalent circuit diagram is shown in Fig. 5e. The following equations are obtained:

$$e_g = i_L R_o + V_D + \frac{1}{C}\int i_L dt \qquad (9)$$

$$e_1 = N e_c \qquad (10)$$

This mode ends at the end of one cycle, $t = T$.

Mode F Core 1 may saturate negative followed by the saturation of core 2, the same consideration must be made as for mode C.

With the substitution of the values of e_s and e_c in the equation, it is seen that the equations for core 1 in Mode A and B are the same as the corresponding equations for core 2 in Mode D and E, except for the sign. The relation between V_A, V_B, V_D, and V_E can be easily obtained by inspection by assuming that neither mode C nor D occur.

$$\begin{aligned} V_B &= V_A - \frac{2}{C} I_m t_{SA} \\ V_D &= -V_B + \frac{1}{C}\int_{t_{SA}}^{T/2} i_{LB} dt \\ V_E &= V_D - \frac{2}{C} I_m t_{SD} \\ V_A &= -V_E - \frac{1}{C}\int_{T/2+t_{SD}}^{T} i_{LE} dt \end{aligned} \qquad (11)$$

A basic equation for magnetic amplifier is one describing the fact that the flux change during the resetting half cycle must be equal to the flux change of the same core during the next gating half cycle; it is true for transient as well as for steady state condition. The flux change may be expressed in terms of the volt-time intregrals and the following equation is obtained:

$$\int_0^{t_{SA}} e_{2A}\,dt + \int_{t_{SA}}^{T/2} e_{2B}\,dt = -\int_0^{t_{SD}} e_{2D}\,dt . \qquad (12)$$

It is well known that the magnetic amplifier is a half-cycle average response circuit and the control voltage of a half cycle has nothing to do with the output of the same half cycle. Therefore, the operation can be described by average values and in the form of a difference equation. Using the subscripts n, n + 1 --- to assign the functions or values to corresponding n, n + 1 half cycles of the source voltage and substituting the values of e_g, e_c, the following difference equations are obtained:

From equations 12, 3, 6, and 7,

$$\left[E_g + V_n - 2I_m R_o - \frac{2}{C} I_m t_{sn}\right] t_{sn} + \left[NE_{cn}\frac{T}{2} - N^2 R_c I_m t_{sn}\right] = \left[E_g + V_{n+1} - 2I_m R_o - \frac{2}{C} I_m t_{sn+1}\right] . \qquad (13)$$

From equation 5, the instantaneous value of i_L in that mode is obtained:

$$i_{LB} = \frac{E_g + V_n - \frac{2}{C} I_m t_{sn}}{R_o} \epsilon^{-\frac{(t - t_{sn})}{\tau}}$$

where $\tau = R_o C$.

And average value of the load current is

$$I_{Ln} = \frac{2}{T}\left[\int_0^{t_{sn}} i_{LA}\,dt + \int_{t_{sn}}^{T/2} i_{LB}\,dt\right] = \frac{4}{T} I_m t_{sn} - \frac{2}{T} C\left[E_g + V_n - \frac{2}{C} I_m t_{sn}\right]\left[1 - \epsilon^{-\frac{(T/2 - t_{sn})}{\tau}}\right] \qquad (14)$$

likewise

$$I_{Ln+1} = \frac{4}{T} I_m t_{sn+1} + \frac{2}{T} C\left[E_g + V_{n+1} - \frac{2}{C} I_m t_{sn+1}\right]\left[1 - \epsilon^{-\frac{(T/2 - t_{sn+1})}{\tau}}\right] . \qquad (15)$$

From equations 11, and 14,

$$V_{n+1} = -V_n + \frac{T}{2C} I_{Ln} . \qquad (16)$$

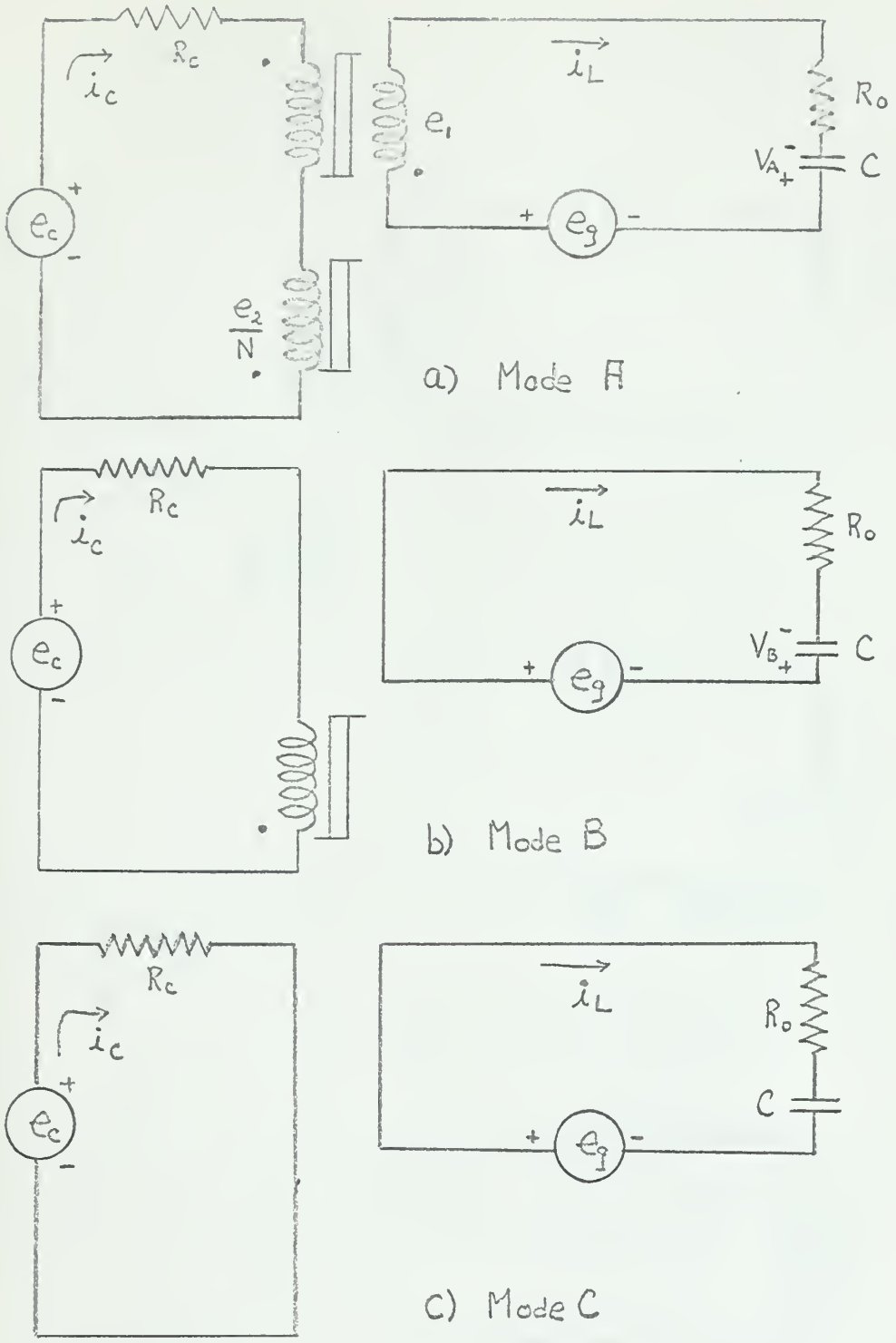

Fig. 5 Equivalent Circuit Diagram in Each Mode

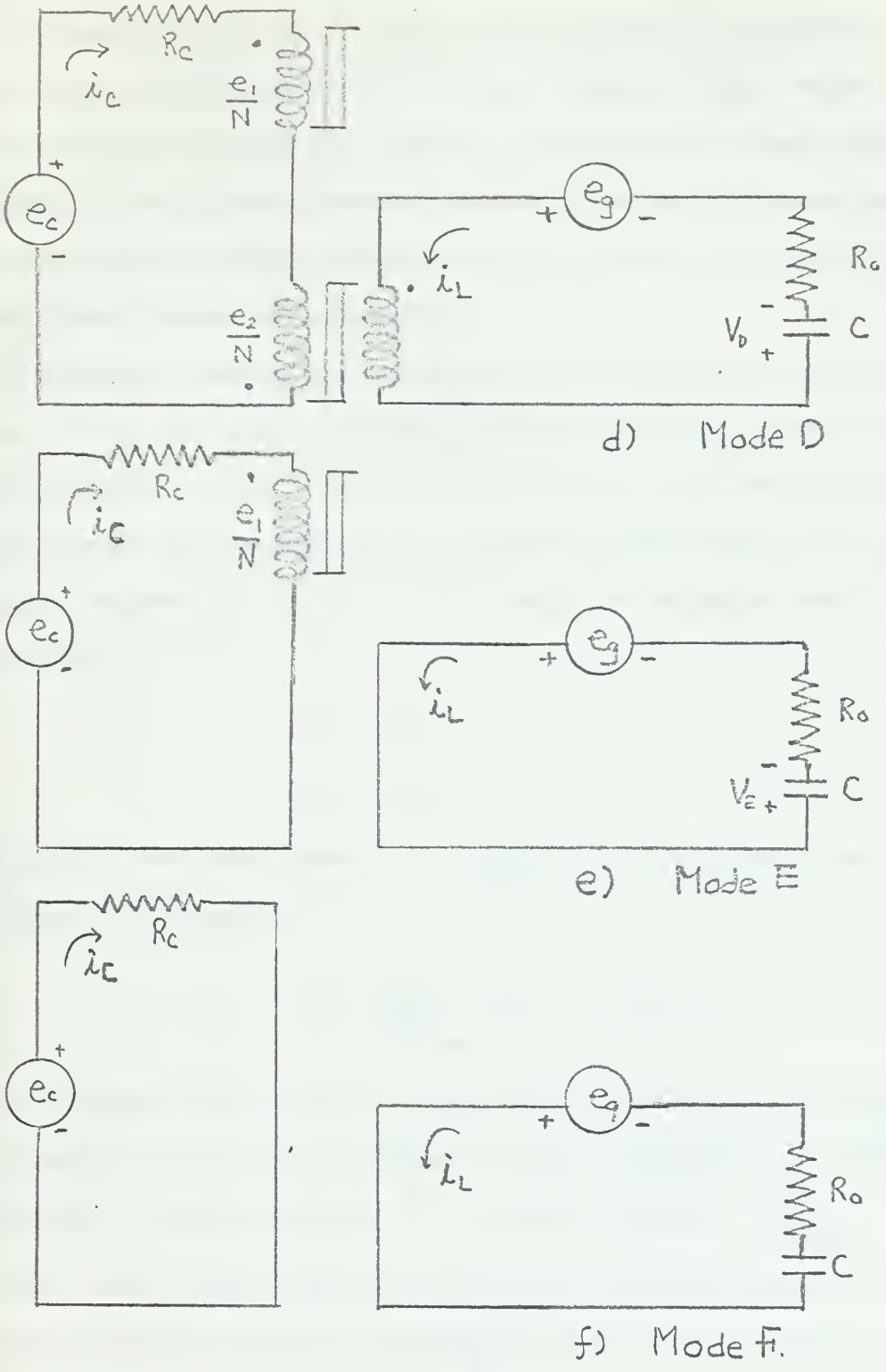

Fig. 5 Equivalent Circuit Diagram in Each Mode

5. Steady State Characteristics

Equations 13, 14, 15, and 16 really describe the operation of this circuit, but they can not be solved to obtain a single output difference equation in terms of I_L and E_c unless they are approximated. Fortunately, even without obtaining an output current difference equation, they may be used to obtain practical and fairly exact results for the steady state transfer characteristics.

The magnetic amplifier is said to be in steady state if the output current of the half cycle is exactly the same magnitude as that of the next half cycle. From equations 14, 15, it is then obvious that the voltage across the capacitor and the saturation time should be the same magnitude for each half cycle, in other words the following conditions must be satisfied:

$$V_m = V_{m+1}$$

$$t_{sm} = t_{sm+1}$$

Substituting these conditions in equation 13, the steady state saturation time may be obtained,

$$t_s = \frac{E_c}{NR_c I_m} \times \frac{T}{2}.$$

Now, it becomes obvious that the sign of control voltage must be negative with respect to the polarity marking of Fig. 1, otherwise it becomes meaningless. For convenience, $\bar{S}$ is used to represent $\frac{E_c}{NR_c I_m}$.

Also, the voltage across the capacitor in the steady state conditions can be easily obtained from equation 16 in terms of output current,

$$V = \frac{T}{4C} I_L$$

By substituting t_s and V in either equation 14 or 15, the load current in the steady state can be obtained in terms of E_g and E_c.

$$I_L = 2\left(\frac{2C}{T}E_g - 2\bar{S}I_m\right)\tanh\left[\frac{T}{4\tau}(1-\bar{S})\right] + \frac{4E_c}{NR_c}\,\frac{1}{\left[1+\epsilon^{-\frac{T}{4\tau}(1-\bar{S})}\right]}$$

The second term of the above equation adds to the complexity of the equation, but inspecting its value in comparison with that of the first term, $\left[1+\epsilon^{-\frac{T(1-\bar{S})}{4\tau}}\right]$ can be very adequately approximated by its maximum value two. With this approximation, the load current is finally obtained.

$$I_L = \left(\frac{4C}{T}E_g - 4\bar{S}I_m\right)\tanh\left[\frac{T}{4\tau}(1-\bar{S})\right] + 2\bar{S}I_m \qquad (17)$$

This steady state transfer equation is only good in the controllable region $0 \leq \bar{S} < 1$. Beyond this region, there is little effect of the capacitor loading and the characteristic becomes almost identical to the characteristic under resistive loads.

The dynamic magnetizing current, I_m, is very important parameter in the above equation, yet it is a function of frequency and the magnitude of applied voltage as pointed out previously.

Manufacturer's data under normal voltage may be used as a first approximation, but better results may be obtained by using the measured I_m under the same voltage as E_g.

Even though it is very complicated, the equation describing load current in the steady state may be derived with a sinusoidal source voltage. In contrast to the case of resistive loading, the modes of operations with sinusoisal source voltage are identical to the corresponding modes with square wave source voltage. As soon as the source voltage swings to positive, mode A starts, due to the voltage across the capacitor which overcomes the forward voltage of rectifier and the IR_o drop in most cases.

The gate voltage is defined as follows in this case:

$$e_g = E_s \sin \omega t - E_f \qquad 0 \le \omega t \le \pi$$
$$= E_s \sin \omega t + E_f \qquad \pi \le \omega t \le 2\pi .$$

From equation 5, the instantaneous value of load current in mode B is obtained, $i_{LB} = \left[\frac{E_s \sin \omega t_{sB} + V_B - E_f - \frac{2}{C} I_m t_{sB}}{R_o} - \frac{E_s}{\sqrt{R_o^2 + (1/\omega C)^2}} \sin(\omega t_{sB} + \varphi)\right] \epsilon^{-\frac{(t - t_{sB})}{\tau}}$

$$+ \frac{E_s}{\sqrt{R_o^2 + (1/\omega C)^2}} \sin(\omega t + \varphi)$$

where $\varphi = \tan^{-1} \frac{1}{\omega \tau}$.

And, the average value of the load current is obtained,

$$I_{Ln} = \frac{4}{T} I_m t_{sn} + \frac{2K_1}{T} \tau \left(1 - \epsilon^{-\frac{(T/2 - t_{sn})}{\tau}}\right) + \frac{4\pi}{T^2} K_2 \left[\cos\varphi + \cos(\omega t_{sn} + \varphi)\right]$$

where

$$K_1 = \left[\frac{E_s \sin \omega t_{sn} + V_n - E_f - \frac{2}{C} I_m t_{sn}}{R_o} - \frac{E_s}{\sqrt{R_o^2 + (1/\omega C)^2}} \sin(\omega t_{sn} + \varphi)\right]$$

$$K_2 = \frac{E_s}{\sqrt{R_o^2 + (1/\omega C)^2}} .$$

The voltage across the capacitor and the saturation time in the steady state are the same as those with a rectangular wave source voltage.

$$V = \frac{T}{4C} I_L$$
$$t_s = \bar{s} \cdot \frac{T}{2}$$

By substituting these, the equation of the load current in the steady state is obtained:

$$I_L = \frac{4}{T} f_1(\bar{s}) \tanh\left[\frac{T}{4\tau}(1 - \bar{s})\right] + \frac{8\pi E_s}{T^2 \sqrt{R_o^2 + (1/\omega C)^2}} f_2(\bar{s}) + 2\bar{s} I_m \qquad (18)$$

where $f_{1(\bar{s})} = CE_s \sin(\pi\bar{s}) - \bar{s} I_m T - CE_f - \frac{E_s \tau}{\sqrt{R_o^2 + (1/\omega C)^2}} \sin(\pi\bar{s} + \varphi)$

$$f_{2(\bar{s})} = \frac{\cos\varphi + \cos(\pi\bar{s} + \varphi)}{1 + \epsilon^{-\frac{T}{2\tau}(1 - \bar{s})}} .$$

The last term is obtained with the same assumption that is applied to the last term of the load current equation with a rectangular wave source voltage. Also, the applicable region is the same, $0 \le \bar{s} < 1$.

Equation 18 clearly shows the complexity of the analysis when sinusoidal source voltage is applied to this circuit.

In deriving the steady state transfer function, it is assumed that the circuit is operating only in modes, A, B, D, and E.

With resistive loading, saturation of both cores can be easily avoided by not applying a source voltage of more than a certain value. This maximum applicable source voltage is called saturation voltage or critical voltage and defined as:

$E_s^* = 4f A_{fe} \beta_s N_g$ for square wave source voltage.

$E_s^* = 4.44 f A_{fe} B_s N_g$ for sinusoidal source voltage.

Indeed, this voltage is the optimum source voltage for resistive loading since maximum power and voltage gain can be obtained.

However, not only the source voltage but also the voltage across the capacitor must be taken into account in the case of capacitive loading, because the voltage across the capacitor contributes along with source voltage in saturating and resetting the cores.

The most pessimistic approach to this would be to limit the source voltage to values such that the sum of the source voltage and the voltage across the capacitor at no control voltage would ever exceed E_s^*.

$$E_s^* = E_g + V = E_g\left[1 + \tanh \frac{T}{4\tau}\right]$$

However, the cores are almost always positively saturated at no control voltage. In other words, mode A, in which the voltage across the capacitor contributes to the reset of the cores, very seldom exists at no control voltage.

If the following inequality is satisfied, the core will not switch from one state of saturation to another during the half cycle, say from positive to negative:

$$E_s^* \frac{T}{2} > (E_g + V_n) t_s .$$

Neglecting the effect of magnetizing current and approximating E_g by E_s,

$$E_s^* > E_s \left[1 + \tanh\left\{\frac{T}{4\tau}(1-\bar{S})\right\}\right]\bar{S} \quad . \qquad (19)$$

If the maximum value of the right side of the above equation with fixed $\frac{T}{4\tau}$ does not exceed E_s^*, the inequality will hold for the entire controllable region, $0 \leq \bar{S} < 1$.

To solve for the maximum value, the right side is differentiated with respect to $\bar{S}$ and the differential is equated to zero. As a result, the following equation is obtained:

$$\frac{T\bar{S}}{4\tau} - 1 = \tanh\left\{(1-\bar{S})\frac{T}{4\tau}\right\} + \frac{T\bar{S}}{4\tau}\tanh^2\left\{\frac{T}{4\tau}(1-\bar{S})\right\}. \qquad (20)$$

The $\bar{S}$ satisfying this equation may be obtained for a given $\frac{T}{4\tau}$, and substituting that $\bar{S}$ in the inequality 19, the critical ratio of E_s^*/E_s may be obtained.

Inspecting the equation, it is evident that no solution exists if $\frac{T}{4\tau}$ is less than one, because maximum $\bar{S}$ is only one. In this case the maximum applicable source voltage is equal to E_s^*. As $\frac{T}{4\tau}$ increases, this voltage approaches the most pessimistic value described previously. Since the solution of equation 19 is tedious, a normalized curve of E_s^*/E_s vs $\frac{T}{4\tau}$ would be valuable. This is shown in Fig. 6.

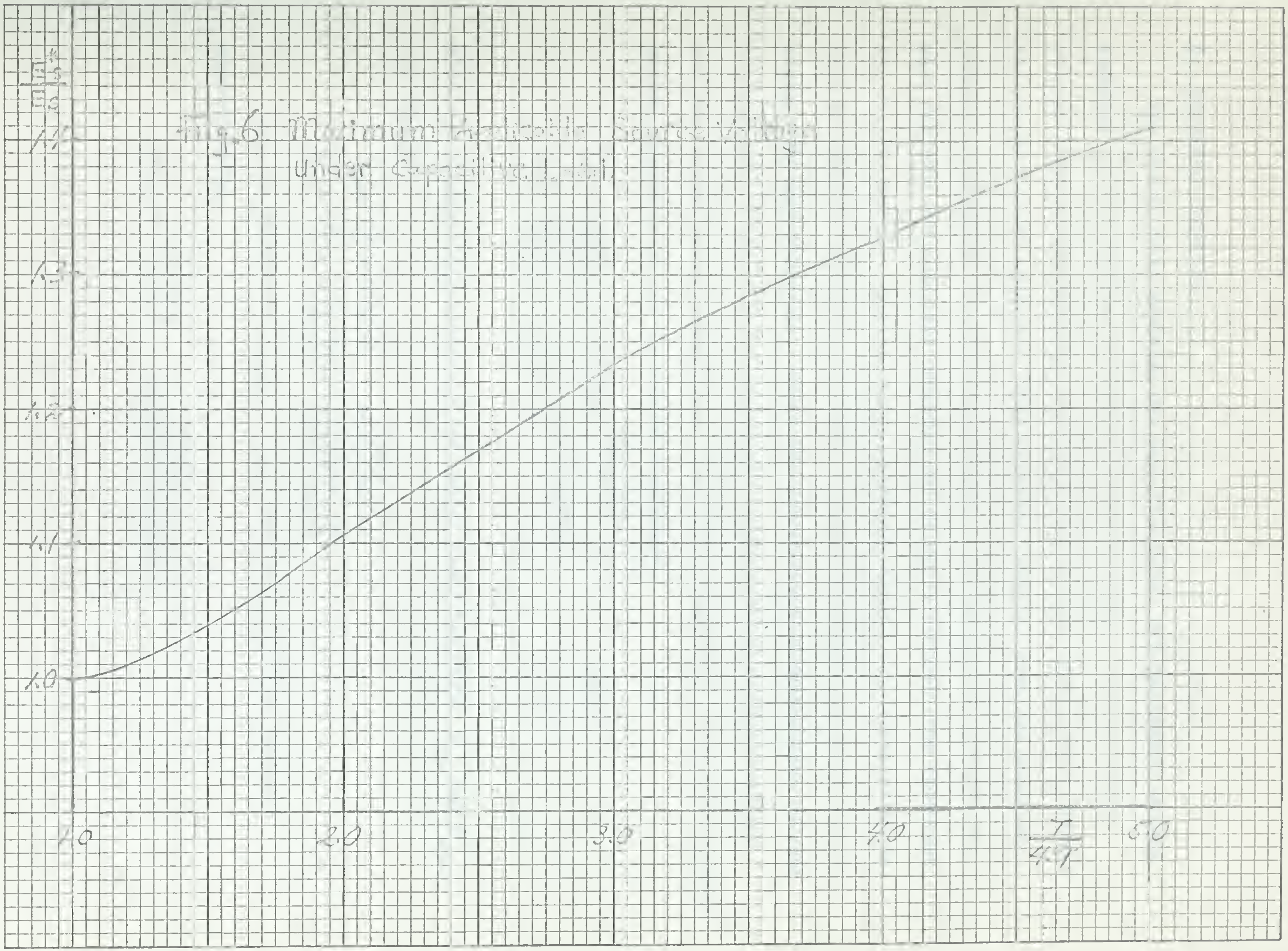

Fig. 6 Maximum [illegible] Source Voltage Under Capacitive Load.

6. Transient Behavior

The steady state behavior has been discussed, and the output current equation has been derived in terms of control voltage. If the control voltage changes, the amplifier will seek a new steady state that satisfies the output current equation. This transient behavior from one state to another is important for some applications. The difference equation can best describe the transient behavior and it may be derived from equations 13, 14, 15, and 16. However, these equations contain non-linear terms so that it would be impossible to obtain a single difference equation without making some approximations. Since the contribution of magnetizing current to equations 14 and 15 is insignificant comparing with the gate voltage and the voltage across capacitance, this can be neglected. With this approximation, equations 14 and 15 will be simplified,

$$I_{Ln} = \frac{2C}{T}\left[E_g + V_n\right]\left[1 - \epsilon^{-\frac{(T/2 - t_{sn})}{\tau}}\right] \qquad (14A)$$

$$I_{Ln+1} = \frac{2C}{T}\left[E_g + V_{n+1}\right]\left[1 - \epsilon^{-\frac{(T/2 - t_{sn+1})}{\tau}}\right]. \qquad (15A)$$

With rearranging these equations and taking their logarithm, t_{sn} and t_{sn+1} are obtained,

$$t_{sn} = \frac{T}{2} + \tau \ln\left[1 - \frac{T I_{Ln}}{2C(E_g + V_n)}\right]$$

$$t_{sn+1} = \frac{T}{2} + \tau \ln\left[1 - \frac{T I_{Ln+1}}{2C(E_g + V_{n+1})}\right].$$

If Δt_s is defined as $t_{sn+1} - t_{sn}$, then Δt_s is also obtained approximately,

$$\Delta t_s \approx \tau \ln\left[1 - \frac{T \Delta I_L}{2C(E_g + V_n) - T I_{Ln}}\right].$$

Substituting equation 16 in it, equation 13 may be rearranged,

$$(E_g - 2I_m R_o)(t_{sn+1} - t_{sn}) - \frac{2}{C} I_m (t^2_{sn+1} - t^2_{sn})$$

$$- V_n (t_{sn+1} - t_{sn}) + \frac{T}{2C} I_{Ln} t_{sn+1} = NE_c \frac{T}{2} - N^2 R_c I_m t_{sn} . \quad (13A)$$

$t^2_{sn+1} - t^2_{sn}$ is approximated to $2\, t_{sn}\, \Delta\, t_s$, and equation 13A may be expressed in terms of output current by substituting t_{sn}, t_{sn+1} and $\Delta\, t_s$.

$$\tau(E_g - 2I_m R_o) \ln\left[1 - \frac{T\Delta I_L}{2C(E_g+V_n) - TI_{Ln}}\right]$$

$$- V_n \left[T + \tau \ln\left\{\left(1 - \frac{T I_{Ln+1}}{2C(E_g + V_{n+1})}\right)\left(1 - \frac{T I_{Ln}}{2C(E_g + V_n)}\right)\right\}\right]$$

$$- \frac{4I_m}{C}\left[\frac{T}{2} + \tau \ln\left(1 - \frac{T I_{Ln}}{2C(E_g+V_n)}\right)\right]\left[\tau \ln\left(1 - \frac{T\Delta I_L}{2C(E_g+V_n) - TI_{Ln}}\right)\right]$$

$$+ \frac{T}{2C} I_{Ln}\left[\frac{T}{2} + \tau \ln\left(1 - \frac{T I_{Ln+1}}{2C(E_g + V_{n+1})}\right)\right]$$

$$= NE_c \frac{T}{2} - N^2 R_c I_m \left[\frac{T}{2} + \tau \ln\left(1 - \frac{T I_{Ln}}{2C(E_g+V_n)}\right)\right] \quad (21)$$

This equation is still nonlinear, and it is found with any further approximations of the equation, accuracy is lost. However the effects of circuit parameters on transient response can be seen qualitatively from the equation. If variation of E_c is very small, the linearization in that range may be possible, but the use of the amplifier under these conditions is notof practical importance.

7. Experimental Results

The experimental results were obtained with the magnetic amplifier which was previously described in section two.

Other circuit characteristics were:

R_g = 27.3 ohms E_f = 1.59 V (Three rectifiers in series)

R_l = 25.6 ohms f = 400 cps

Three magnitudes of source voltage were used, E_s = 12, 15, and 22 volts. R_L was either 500 ohms or 1000 ohms, also various magnitudes of R_c were used to assure that normalization to $\bar{S}$ was approximately correct. The magnetizing current, I_m, with normal sinusoidal exciting voltage was .44ma, but it depends on voltage and from the experiment the following results were obtained:

$$I_m = .25 \text{ ma} \quad \text{with} \quad E_s = 22\text{v}$$

$$= .20\text{ma} \quad \text{with} \quad E_s = 15\text{v} .$$

The source voltage was obtained with a magnetic-transistor inverter. Fig. 7 a and b show wave forms of load current, control current, the voltage across the capacitor, the induced emf, and the voltage drop across the rectifier. From these assumptions and modes of operation become clearer, Fig. 7c illustrates mode c.

Steady Stat Characteristics

Figs. 8 and 9 compare the calculated and experimental results to verify equation 17. Even though the calculated results from equation 17 do not match with experimental, they are reasonably close, considering the limitation of the applicable source voltage except for near the end of the curves where a bivalue characteristic exists. Also it is observed that the smaller the source voltage is compared with E_s*, the more widely the results differ.

Fig. 9 shows the case in which mode C operation is involved during the cycle. As soon as this occurs, the load current holds almost constant until the control voltage reaches a certain value. At this moment the load current switches to a very small value.

The mechanism of this switching is not clear, but apparently the voltage across the capacitor starts to collapse at this moment due to the increased magnitude of magnetizing current in mode A operation. Once started the load current switches within a few cycle.

The bivalue characteristic which is sometimes referred to as "jumping" is encountered in the steady state characteristic. This becomes more apparent when the source voltage is far less than E_s^*. The theory about this phenomena has been discussed by Bartdorf and Johnson, dealing with the half-wave magnetic amplifier and resistive loading. [7] In the controllable region, one of the cores is in positive saturation at the end of a half cycle. But once the load current reaches a minimum and if E_c is increased further, neither of the cores reaches positive saturation, and when E_c is reduced, the load current will not follow the previous curve, but continuously decreases as E_c is decreased. This is continued until one of the cores reaches positive saturation, against the reluctance due to domain movement. This explanation is clarified by the fact that when the load current reaches a minimum value and E_c is decreased immediately, the load current follows the major curve and does not show the bivalue characteristics if τ is fairly large. If τ is small, the effect of the voltage across the capacitor becomes greater and as soon as the load current reaches the minimum value, neither core reaches positive saturation in the next half cycle.

It should be pointed out that this phenomena occurs only when the gate voltage is less than E_s^*, and this is most the likely case with capacitive

loading.

One of the interesting phenomena with this circuit is the oscillation of load current when the load current is near its minimum value. Some of these oscillations with various values of τ and E_c are shown in Figs. 10 and 11. The oscillations in the middle range of E_c are fairly periodic, but some of them are very irregular.

The mechanism of this oscillation is not clear, and it is felt that further understanding of the core behavior in this range is needed to explain this oscillation.

Transient Response

As equation 21 implies, the transient behaviour was very complicated, and only a qualitative trend could be presented. The rising transient response was quite different from the decaying response in terms of the time taken to reach steady state as well as in response wave form. In each case, the effects of circuit parameters were examined qualitatively. The time constant in this section is defined as the time taken to reach 63% of the new steady state value from the original value. Since the responses were not necessarily exponential, it gave only a qualitative measure of the responses.

In rising, the following trends were observed:

(1) A larger source voltage resulted in a longer time constant, as shown in Figs. 12a, b, and c.

(2) A larger τ resulted in a longer time constant, as shown in Figs. 12, d, e, g, and h. When "jump" occured in the response, a longer settling time was taken even though the time constant was very small.

(3) When the load current rose from a large control voltage, a shorter time constant was obtained. If control voltage was too large, there was a delay before rising. The rising portion of the response remained identical to each other regardless of the amount of delay. Figs. 12a, d, e, and f show the examples.

The decaying transient usually took a longer time than the rising transient except in the case when the control voltage was very large. In this case decaying was less like an exponential. The source voltage had the same effect on time constant as in the case of rising transient as shown in Figs. 13a and b. Figs. 13 d and c show the effect of τ on the response; as τ increased the time constant increased. If τ was so small that mode C operation existed, the above trend no longer held, as shown in Figs. 13 g and h. A larger control voltage resulted in a shorter time constant. Figs. 13 e and f show this effect; the responses are almost straight lines.

Magnetic amplifiers have inherently a half-period delay as previously mentioned. In addition to this, it was observed that there was a long delay before rising if a larger control voltage was applied and suddenly removed than the one that was needed for the load current to reach its minimum value. This phenomena can be explained by the same theory that explained "jump" in steady state characteristics. It took time for one of the cores to reach positive saturation even if the control voltage was removed.

Fig. 14 shows some of the long delays, and by comparison the effect of circuit parameters could be deduced. Even though it was not feasible in this paper to relate delay time numerically with other circuit parameters, some qualitative relations could be stated:

(1) As the source voltage approached E_s^*, delay time became shorter

with given $\bar{S}$ and τ , also the source voltage determined the longest delay time.

(2) The control voltage, and $\bar{S}$ in turn was the prevailing factor within the limit set by the source voltage; the larger E_c was, the longer the delay time was. But the delay time was not proportional to E_c, rather it approached exponentially to a limit.

(3) The delay time was fairly independent of τ , but the delay time slightly decreased as τ became smaller.

(4) The length of delay time was also dependent upon how long E_c was continuously applied. It was noticed in measurement that delay time gave a somewhat wide statistical distribution, if the source voltage was far less than E_s*, since it was easily subjected to noise.

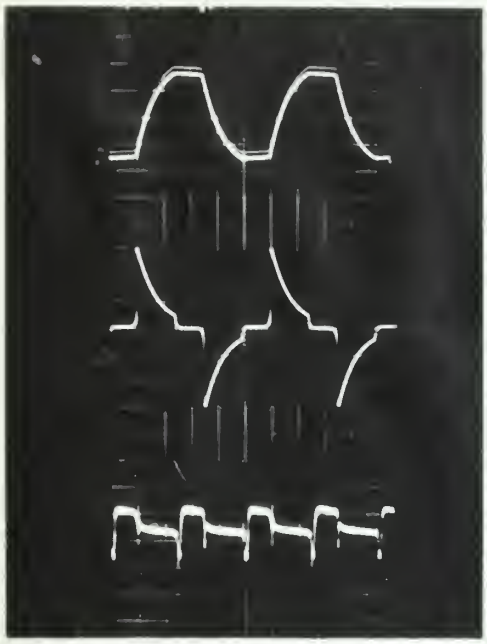

(a)

(b)

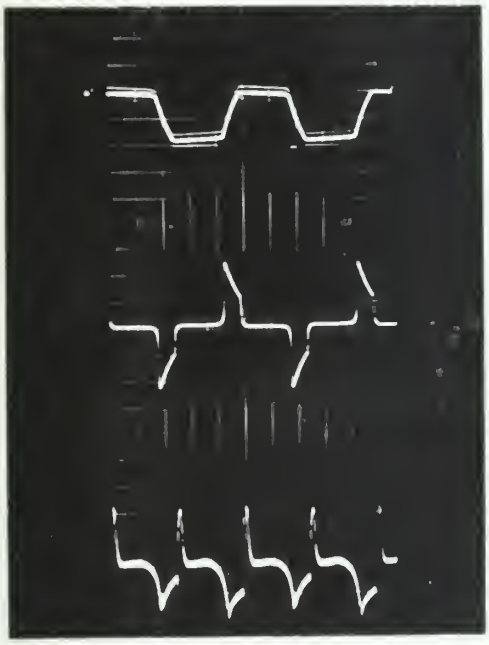

(c)

Fig. 7 Wave Forms of i_L, i_C, V, e_l, and Voltage drop across a rectifier.

a) and b) with small E_C

c) with large E_C

a) c) Top — V

Center — i_L

Bottom — i_e

b) Top — e_l

Bottom — Voltage drop across a rectifier

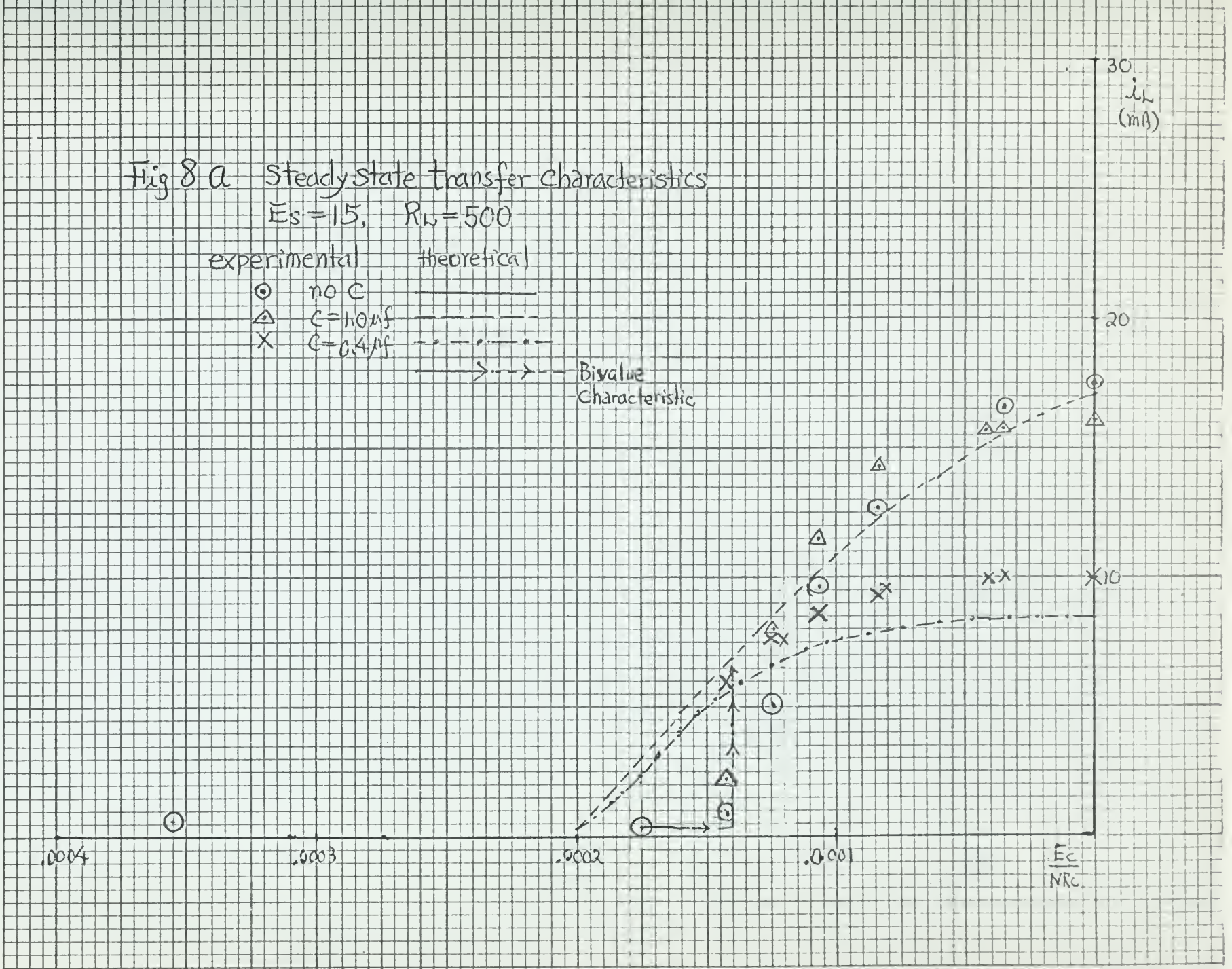
Fig 8 a Steady state transfer characteristics
Es = 15, RL = 500
experimental
theoretical
no C
C = 10 μf
C = 0.4 μf
Bivalue Characteristic
30
20
10
iL (mA)
.0004
.0003
.0002
.0001
Ec / NRc

Fig. 8b Steady state transfer characteristics

$E_s = 15$ V, $R_L = 100\Omega$

experimental		theoretical
⊙	$C = 1.0\,\mu f$	———
×	$C = 0.5\,\mu f$	— — — —
△	$C = 0.2\,\mu f$	— · — · —
Bivalue Characteristic		→ → →

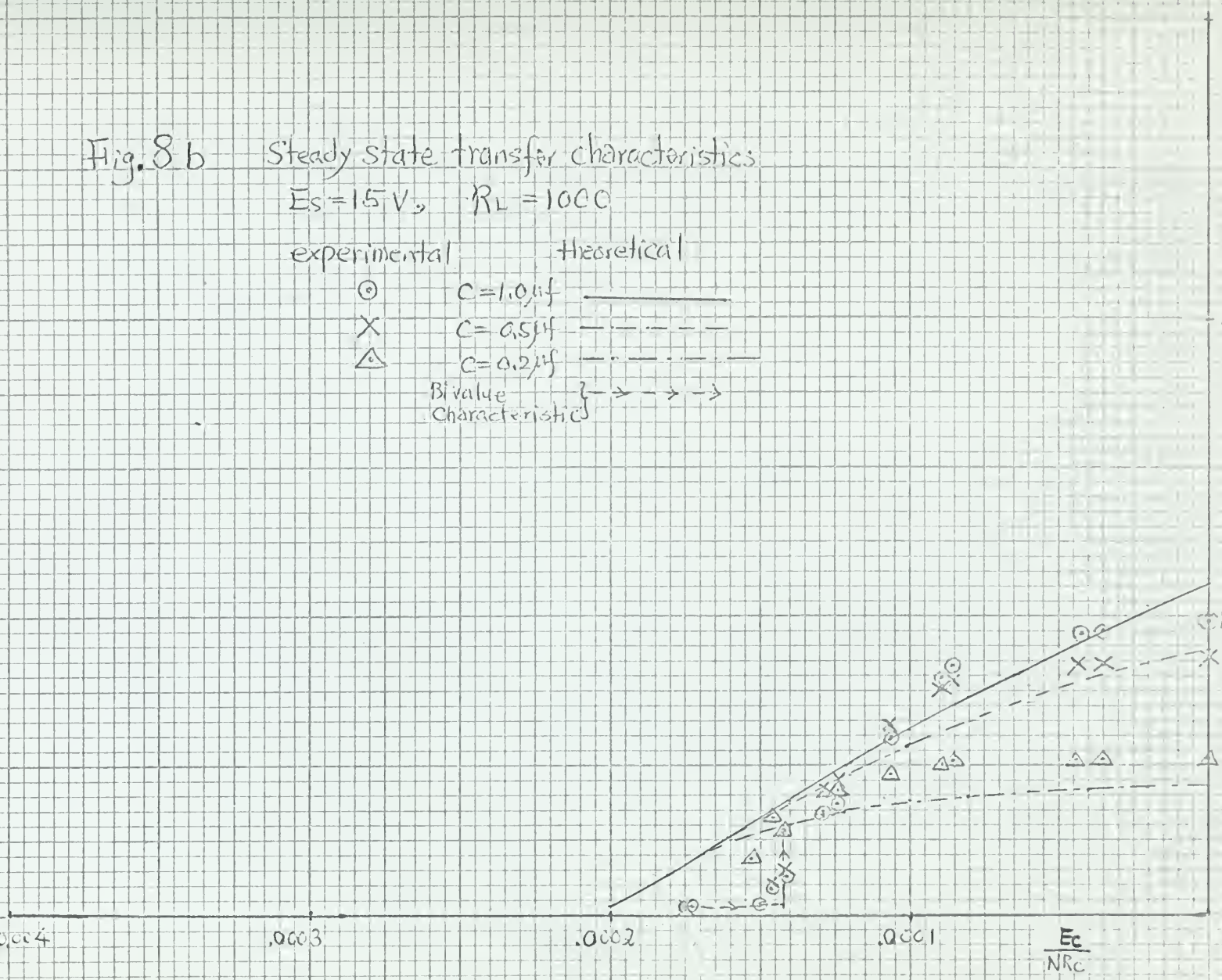

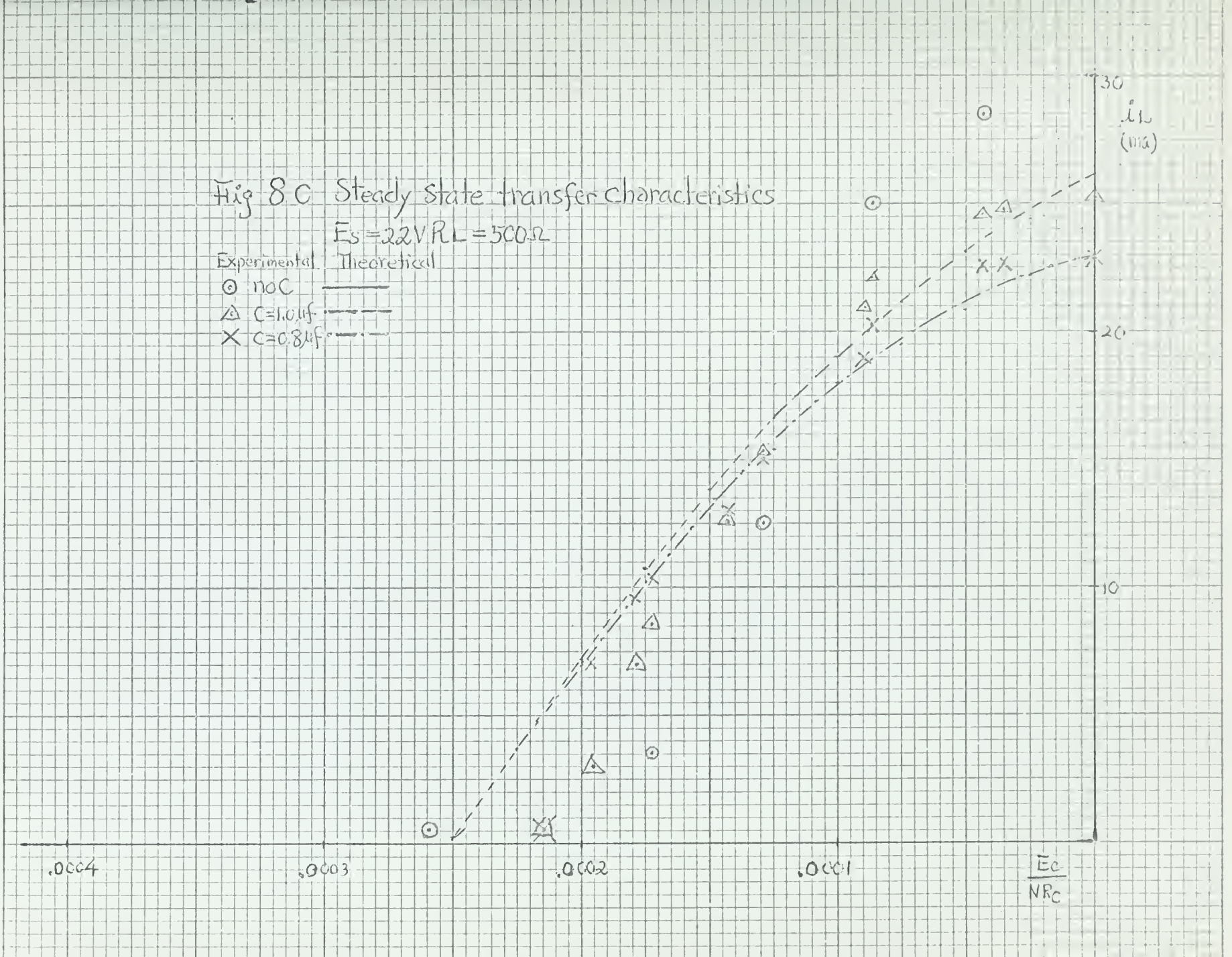
Fig 8 C Steady state transfer characteristics
Es = 22V RL = 500Ω
Experimental Theoretical
⊙ no C
△ C = 1.0 μf
× C = 0.8 μf
30
20
10
i_L (ma)
.0004
.0003
.0002
.0001
$\frac{E_c}{NR_c}$

Fig. 8d Steady State transfer characteristics
$E_s = 22\,V$, $R_L = 1000\,\Omega$

Experimental — Theoretical
- ⊙ C = 1.0 μf ——
- △ C = 0.5 μf - - - -
- X C = 0.4 μf — · —

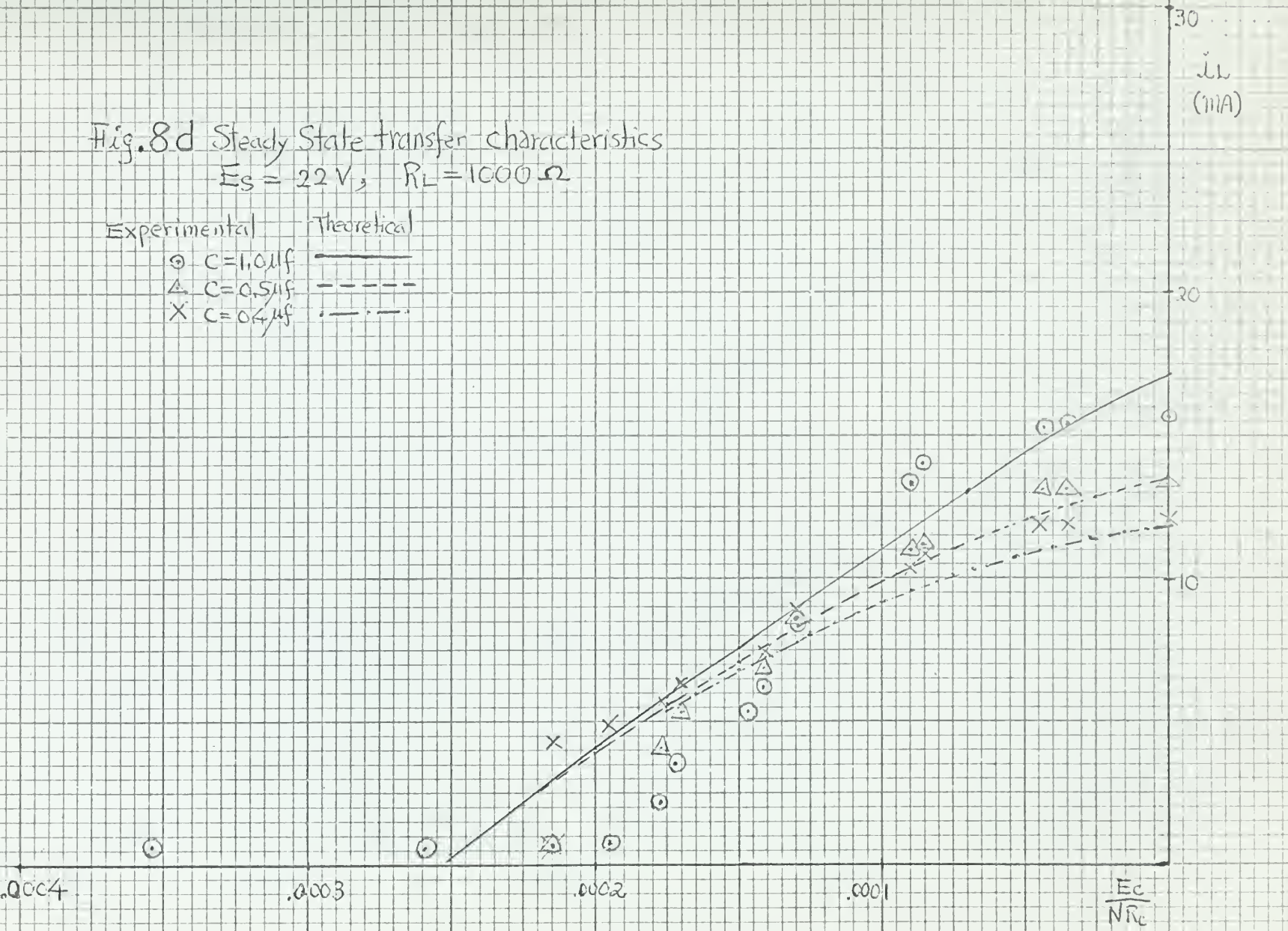

Fig. 9 Steady State transfer characteristic
With hysterisis loop. $E_s = 22$

Experimental — Calculated

- - ⊙ - - - $R_L = 500$ $C = 0.6\,\mu f$ ——
- - X - - - $R_L = 1000$ $C = 0.3\,\mu f$. ——

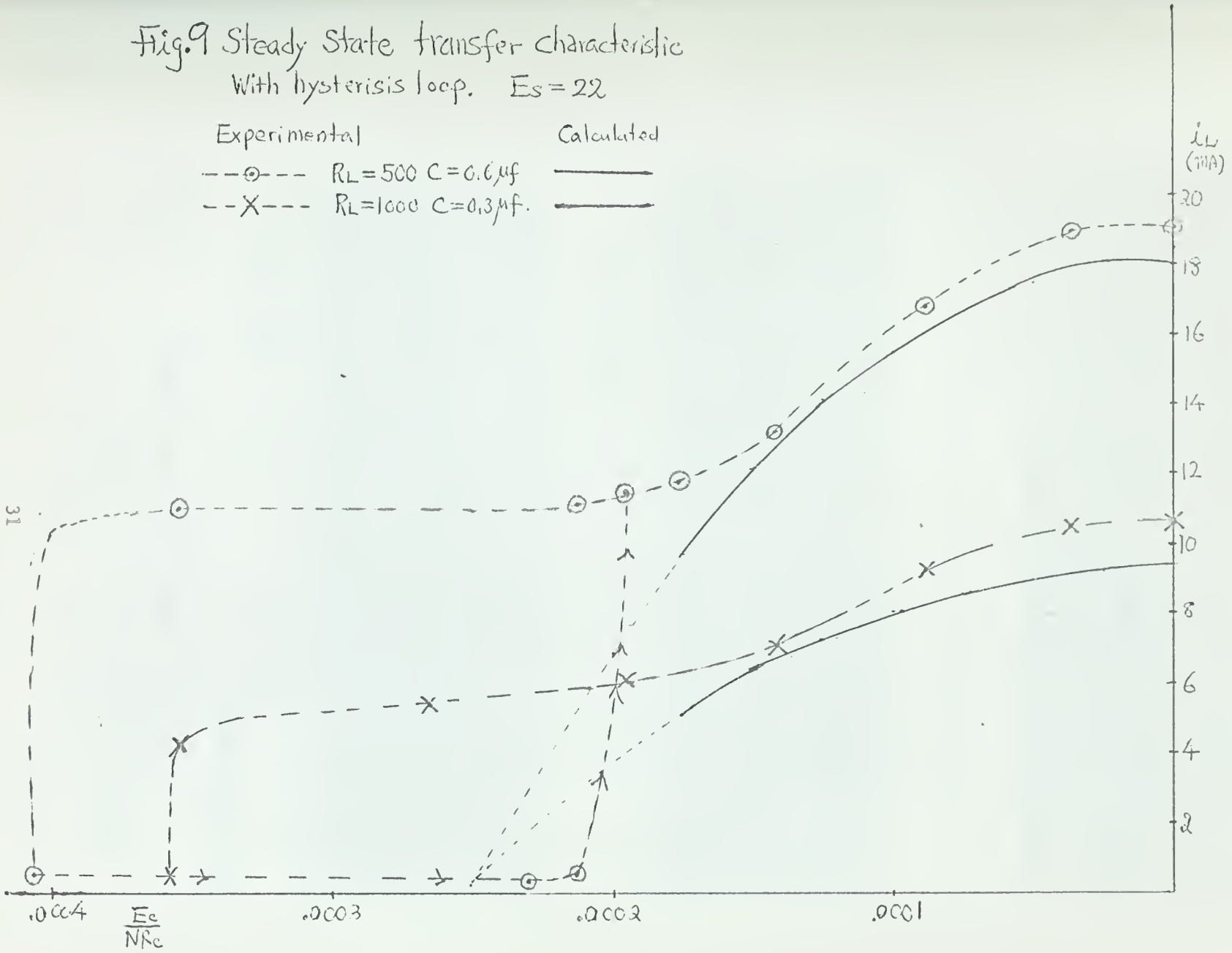

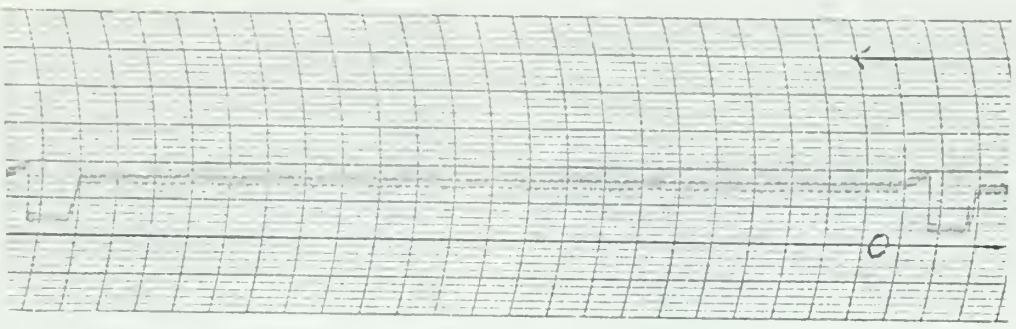

a) $E_c = 0.170$ V
$C = 0.2\,\mu f$

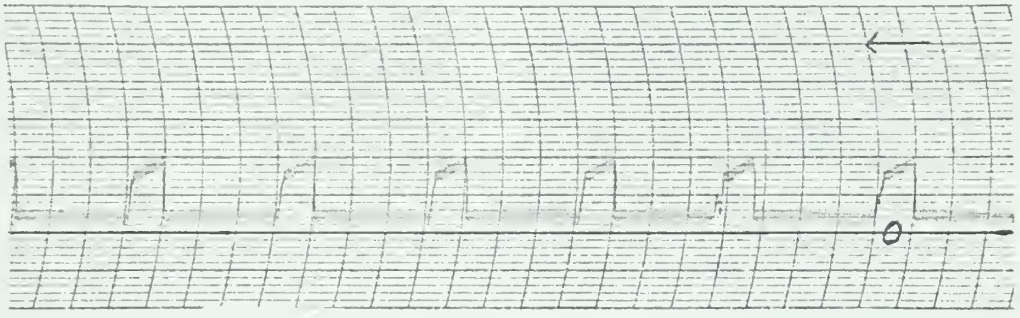

b) $E_c = 0.172$ V
$C = 0.2\,\mu f$

c) $C = .5\,\mu f$
$E_c = .158$ V

$C = .5\,\mu f$
$E_c = .155$ V
(timescale 25 mm/sec)

Fig. 10 Oscillogram of Load Current.
with $E_{sr} = 15$ V $f = 400$ cps (sinusoidal)
$R_L = 500\,\Omega$ $R_c = 582.6\,\Omega$

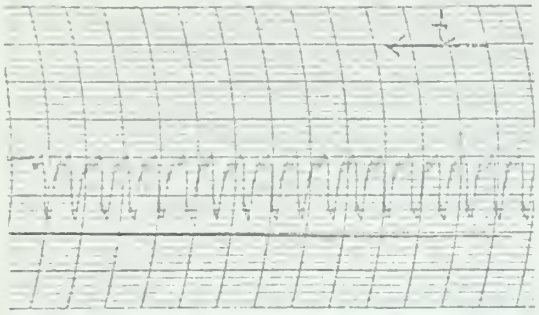

(a) $C = .4\,\mu f$ $E_c = .155$

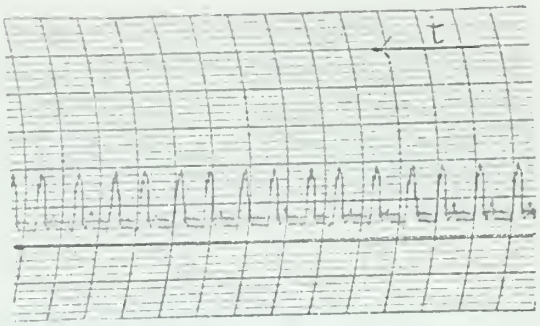

(b) $C = .4\,\mu f$ $E_c = 0.162$

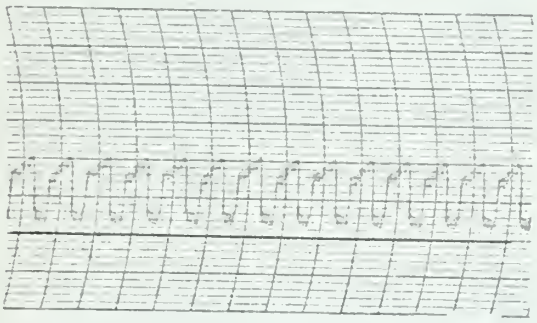

(c) $C = .3\,\mu f$ $E_c = 0.16$ V

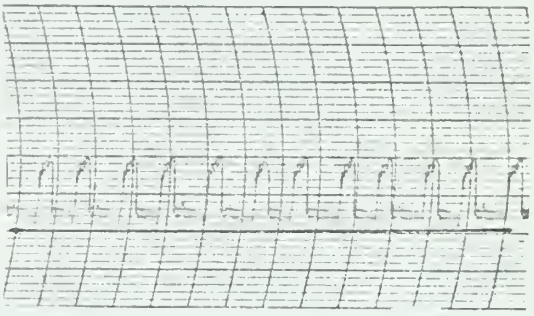

(d) $C = .3\,\mu f$ $E_c = .165$ V

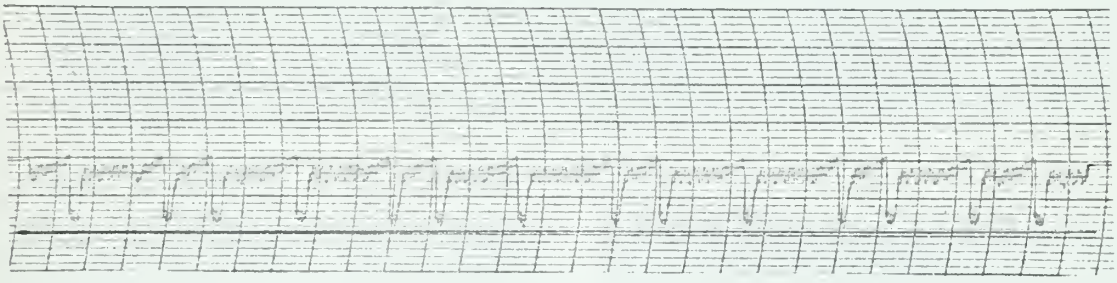

(e) $C = .3\,\mu f$ $E_c = 0.155$ V

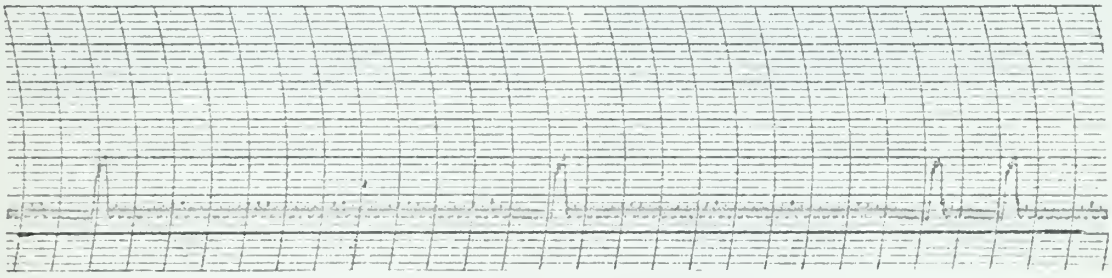

(f) $C = .3\,\mu f$ $E_c = .169$ V

(time Scale 25 mm/sec)

Fig. 10 Oscillation of Load Current
with $E_{s_f} = 15$ V $f = 400$ cps (sinusoidal)
$R_L = 500\,\Omega$ $R_c = 582.6\,\Omega$

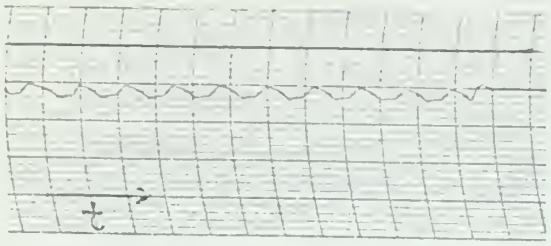

(a) $C = .8\,\mu f$ $E_c = .179\,V$

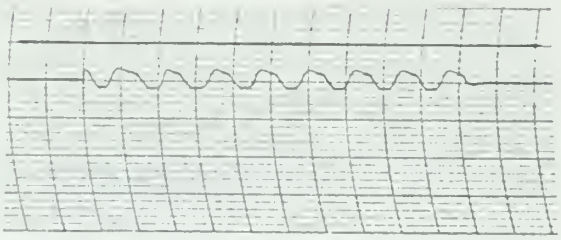

(b) $C = .8\,\mu f$ $E_c = .18\,V$

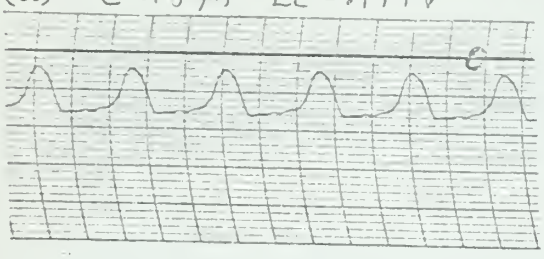

(c) $C = .5\,\mu f$ $E_c = .180\,V$

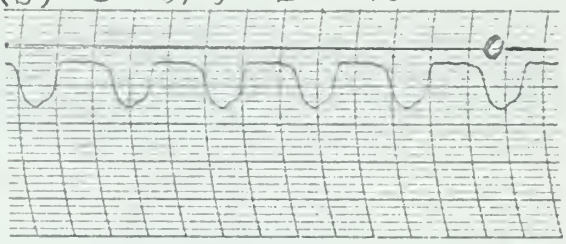

(d) $C = .5\,\mu f$ $E_c = .185\,V$

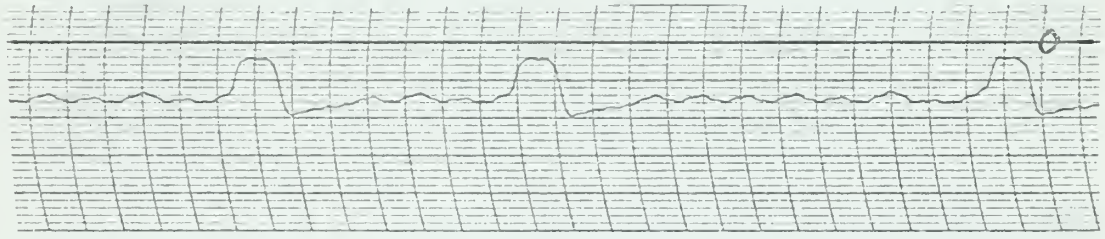

(e) $C = .4\,\mu f$ $E_c = .183\,V$

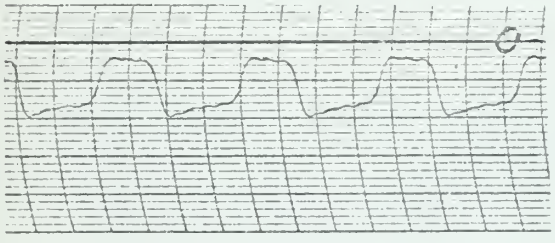

(f) $C = .4\,\mu f$ $E_c = .185\,V$

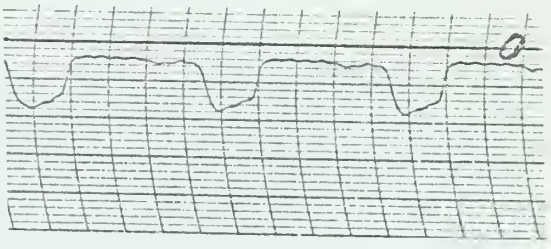

(g) $C = .4\,\mu f$ $E_c = .190\,V$

(time scale 125 mm/sec)

Fig. 11 Oscillation of Load Current
with $E_{s_r} = 20V$ $f = 400$ cps (sinusoidal)
$R_L = 500\Omega$ $R_c = 582.6\,\Omega$.

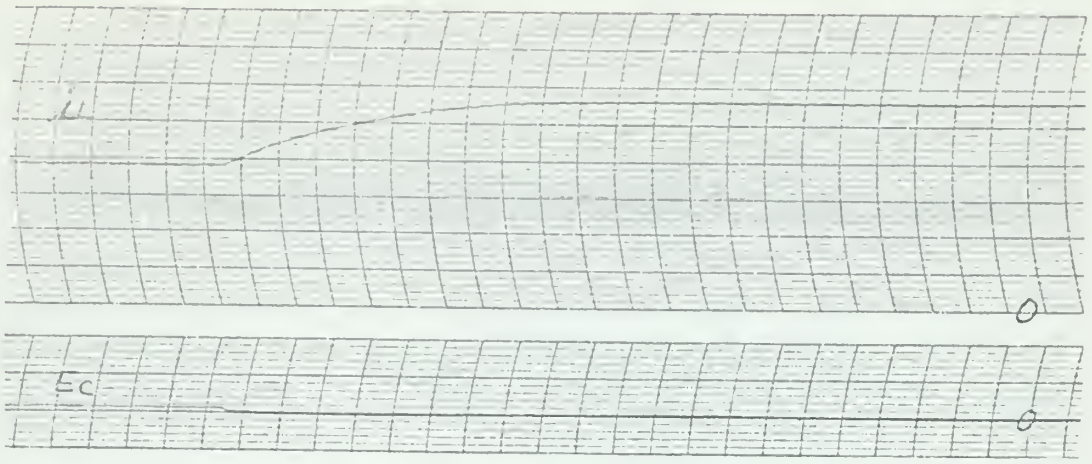

a) $E_s = 22\,V$, $R_c = 132\,\Omega$, $R_L = 500\,\Omega$, $C = 1.0\,\mu f$, $E_c = 0.03\,V$, T.C. = 136 msec

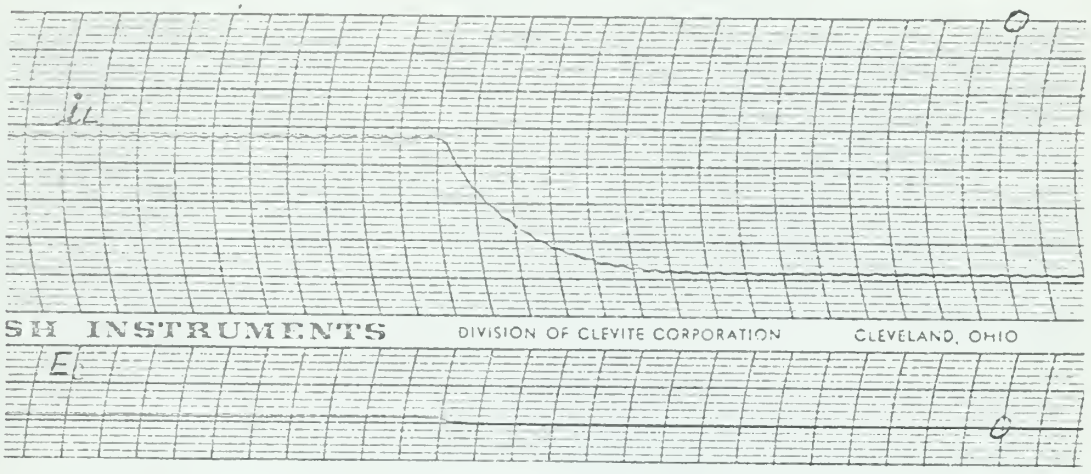

b) $E_s = 15\,V$, $R_c = 132\,\Omega$, $R_L = 500\,\Omega$, $C = 1.0\,\mu f$, $E_c = 0.03\,V$, T.C. = 76 msec

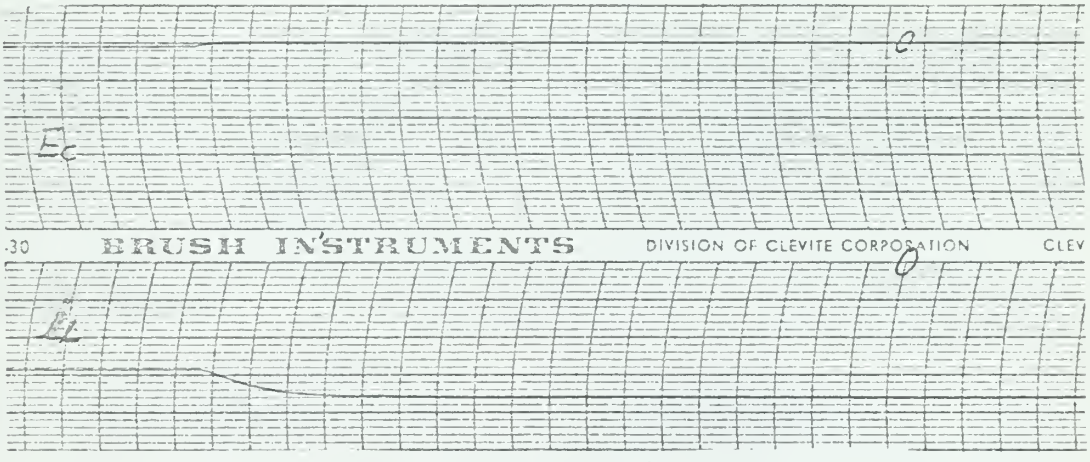

C) $E_s = 12\,V$, $R_c = 132\,\Omega$, $R_L = 500\,\Omega$, $C = 1.0\,\mu f$, $E_c = 0.025\,V$, T.C = 56 msec.

Fig. 12 Transient Response (Rising)

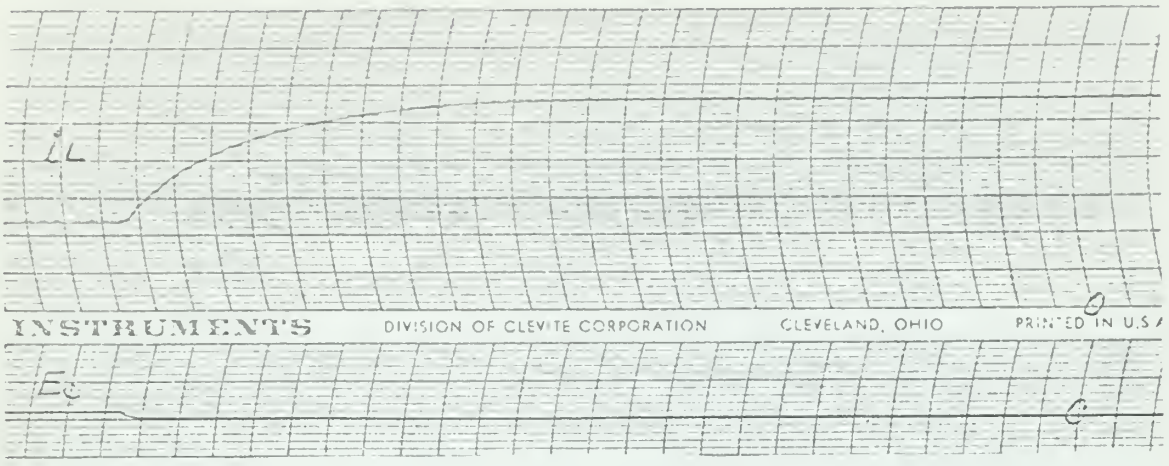

d) $E_S = 22V$ $R_L = 500\Omega$ $E_c = 0.04V$ $C = 1.0\mu f$ T.C. = 128 msec

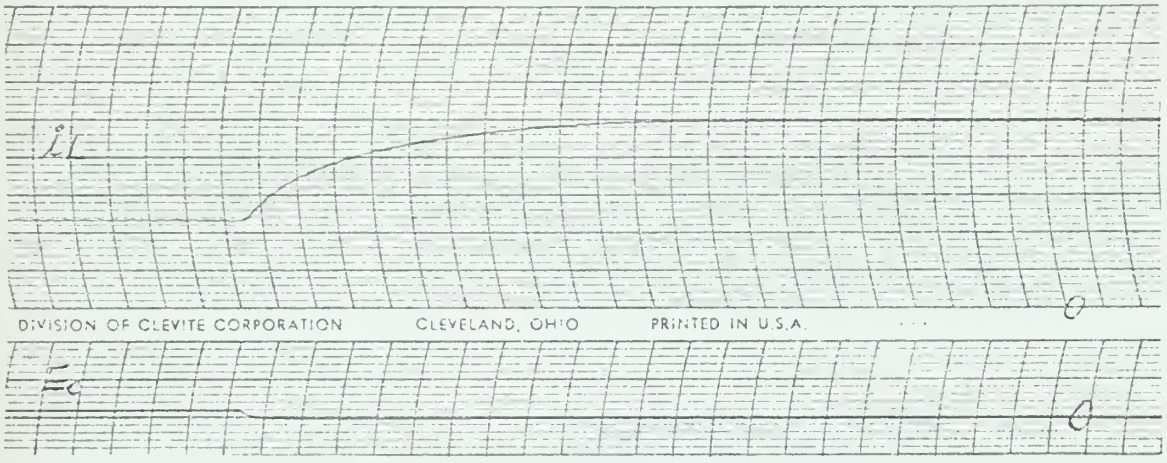

e) $E_S = 22V$ $R_L = 500\Omega$ $E_c = 0.04V$ $C = 0.8\mu f$ T.C. = 122 msec.

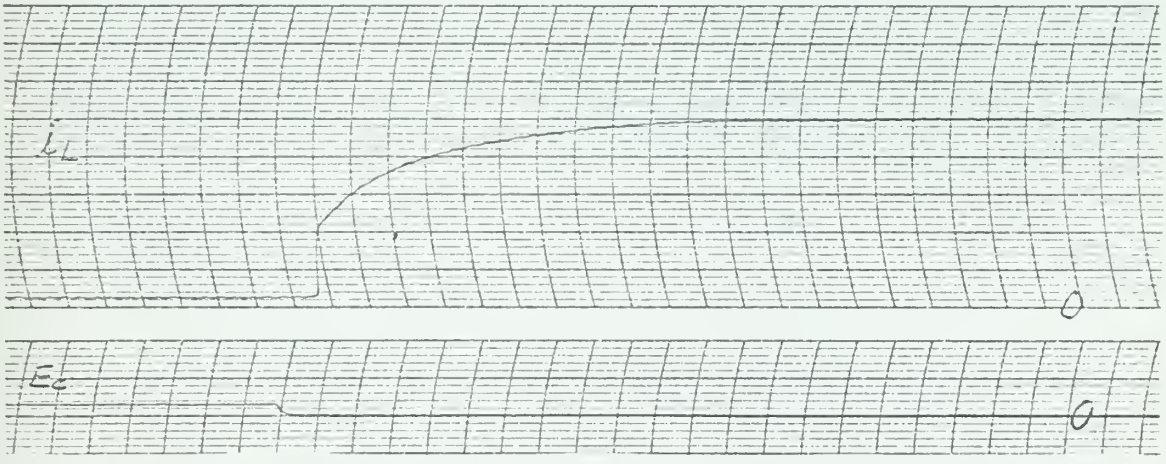

f) $E_S = 22V$ $R_L = 500\Omega$ $E_c = 0.065V$ $C = .8\mu f$ T.C. = 68 msec.

Fig. 12 Transient Response (Rising)

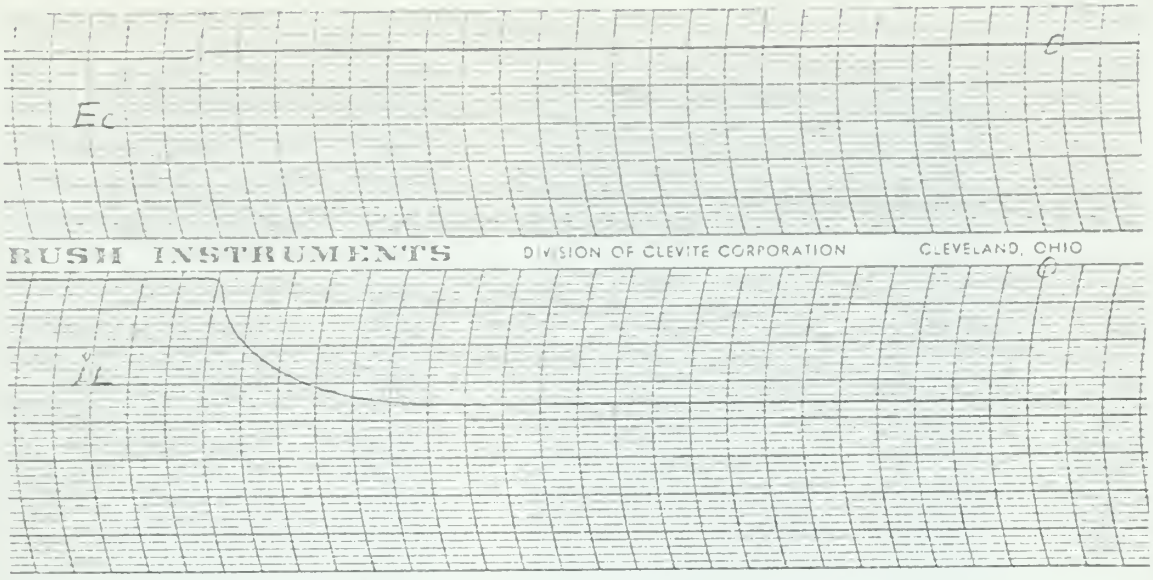

g) $E_S = 12\,V$ $R_c = 132\,\Omega$ $R_L = 500\,\Omega$ $C = 1.0\,\mu f$ $E_c = 0.035\,V$
T.C. = 56 msec

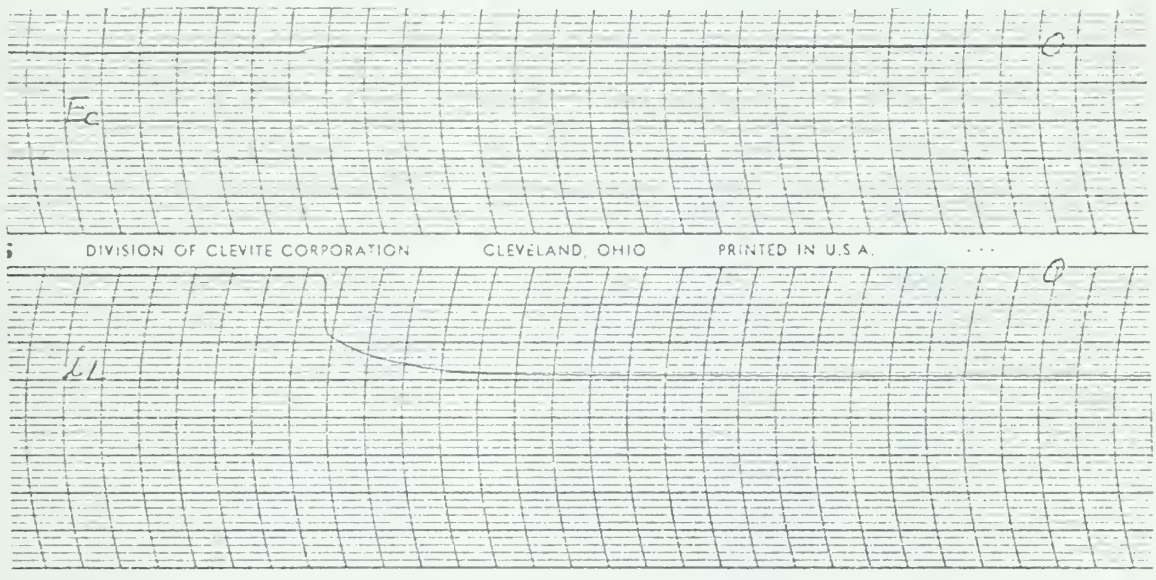

h) $E_S = 12\,V$ $R_c = 132\,\Omega$ $R_L = 500\,\Omega$ $C = 0.6\,\mu f$ $E_c = 0.035\,V$
T.C. = 22 msec

Fig. 12. Transient Response (Rising)

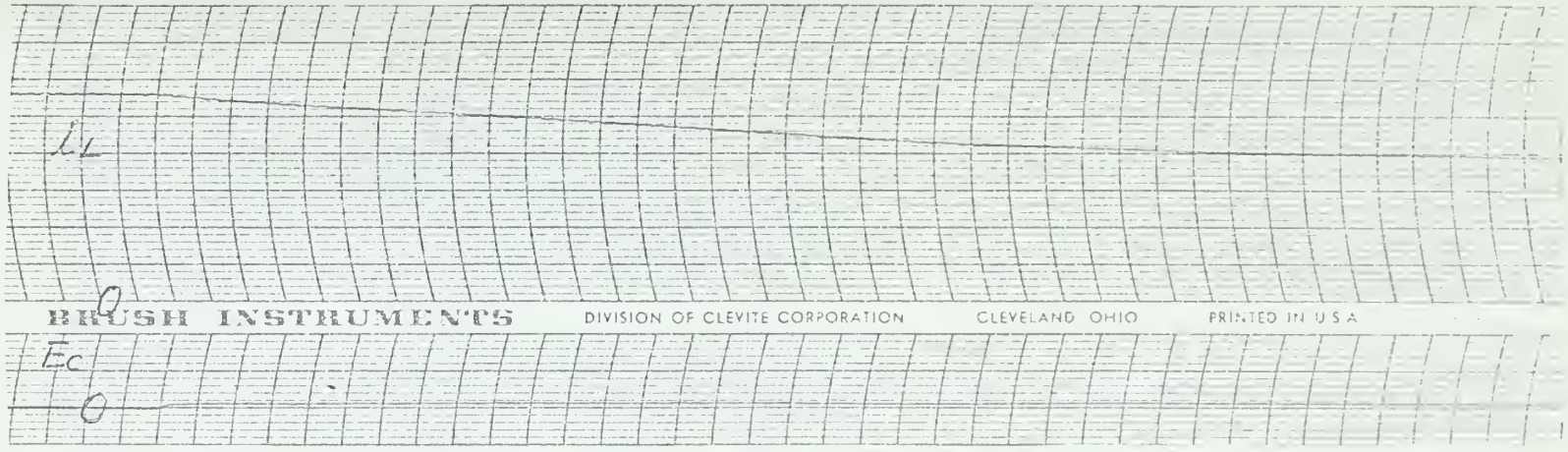

a) $E_s = 22\,V$ $R_c = 132\,\Omega$ $R_L = 500\,\Omega$ $C = 1.0\,\mu f$ $E_c = 0.03\,V$ T.C = 728 msec

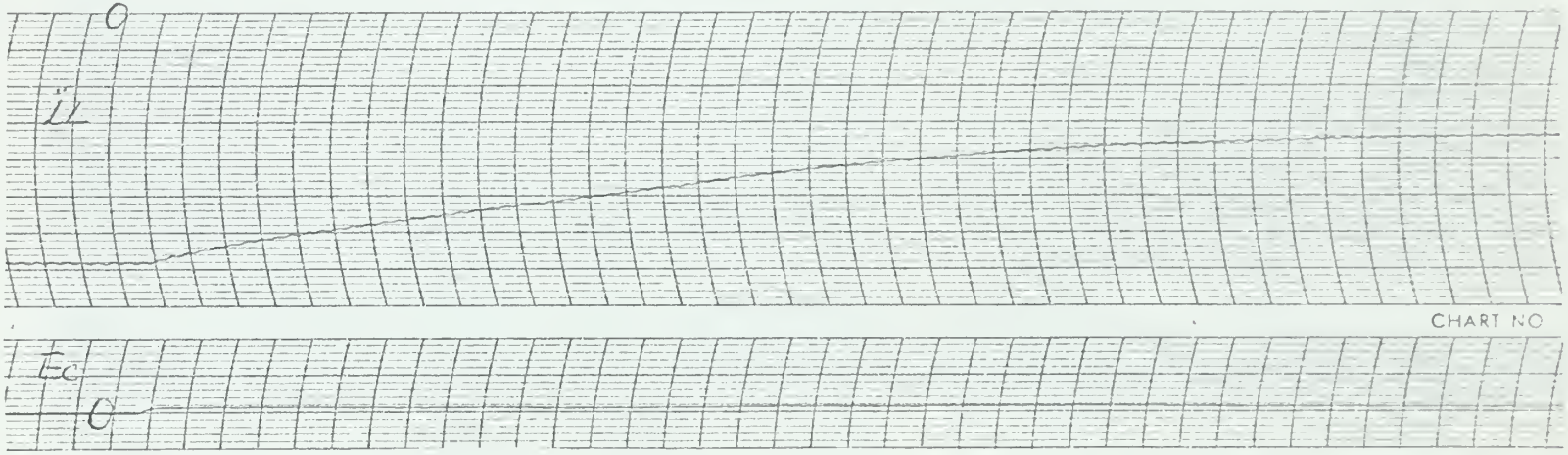

b) $E_s = 15\,V$ $R_c = 132\,\Omega$ $R_L = 500\,\Omega$ $C = 1.0\,\mu f$ $E_c = 0.03\,V$ T.C. = 588 msec.

Fig. 13 Transient Response (Decaying)

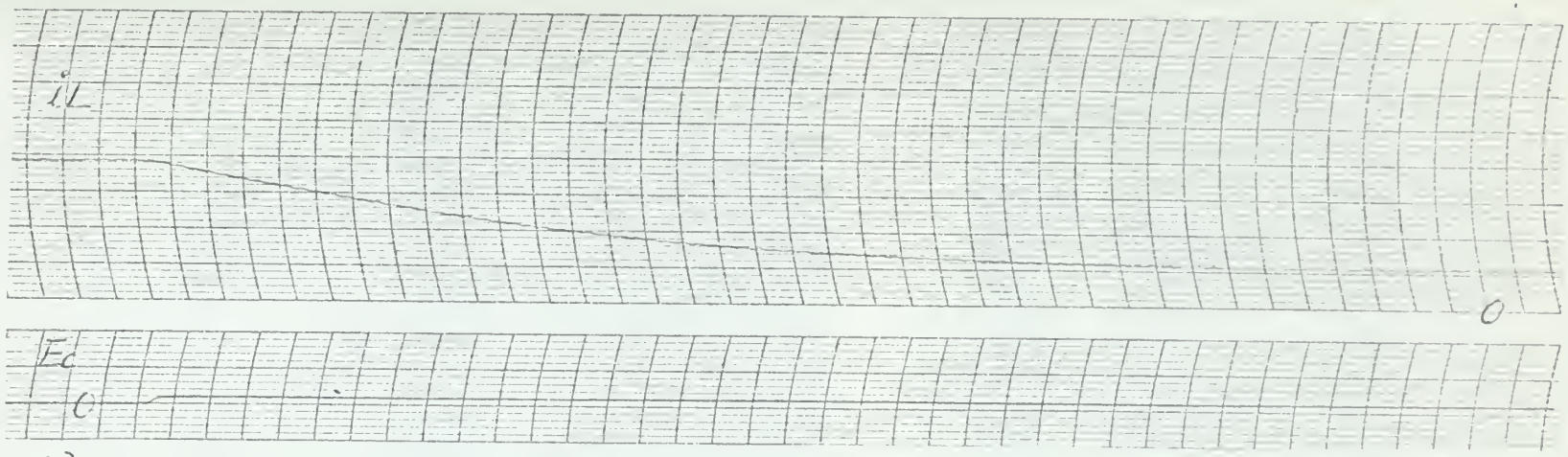

C) $E_s = 22\,V$ $R_L = 1000\,\Omega$ $C = 1.0\,\mu f$ $R_c = 132\,\Omega$ $E_c = 0.04\,V$ $T.C. = 434\,msec$

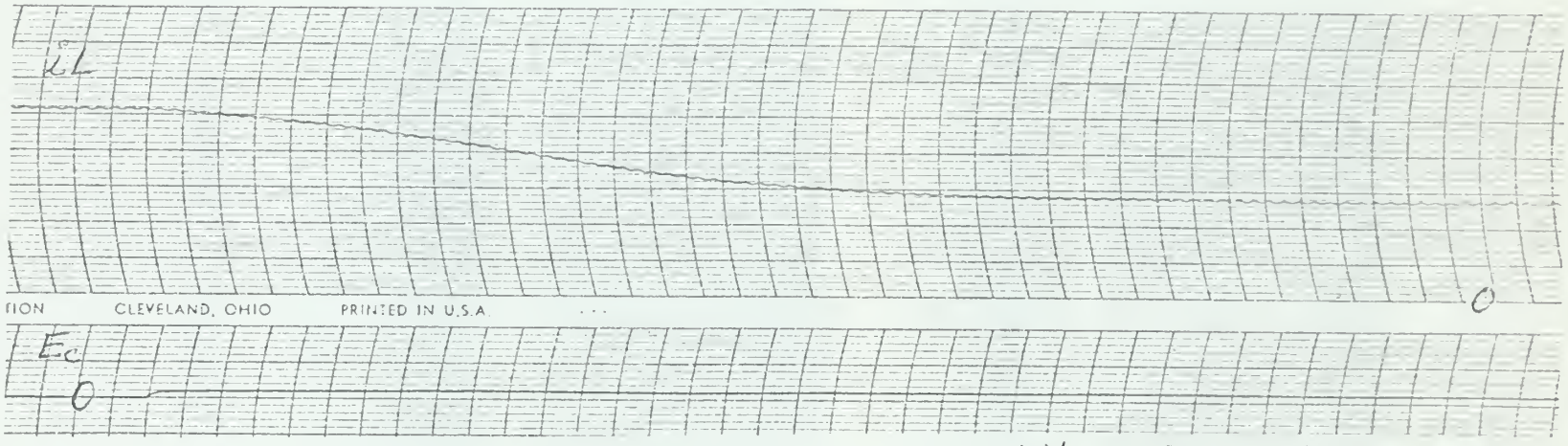

d) $E_s = 22\,V$ $R_L = 1060\,\Omega$ $C = 0.4\,\mu f$ $R_c = 132\,\Omega$ $E_c = 0.04\,V$ $T.C. = 504\,msec$

Fig. 13 Transient Response (Decaying)

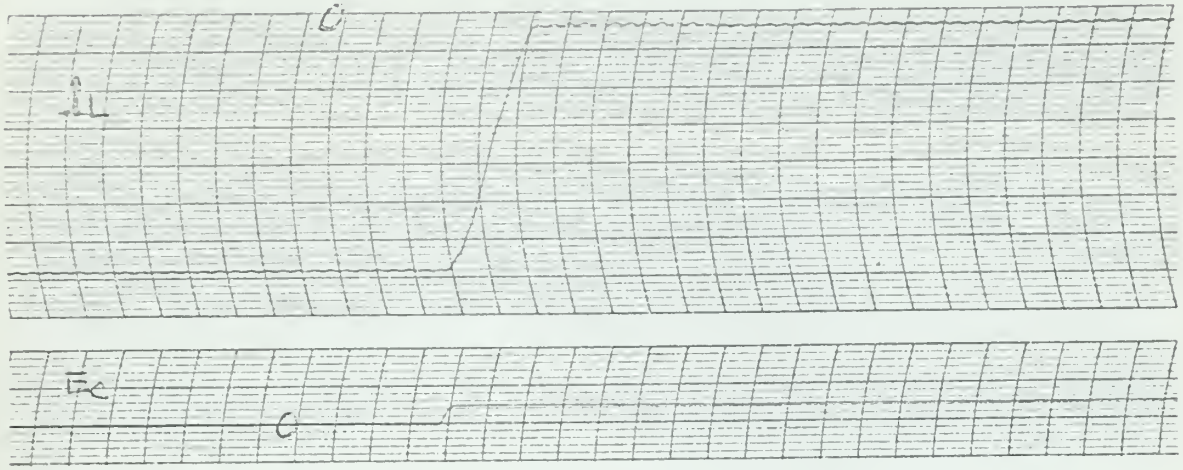

e) $E_s = 15V$ $R_L = 500\Omega$ $C = 1.0\mu f$ $R_c = 132\Omega$ $E_c = 0.1\,V$

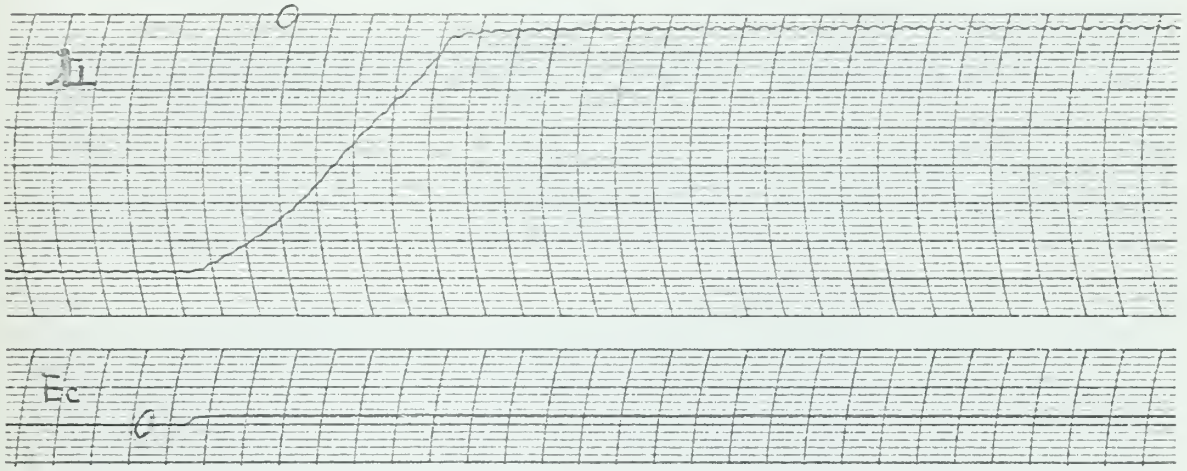

f) $E_s = 15V$ $R_L = 500\Omega$ $C = 1.0\mu f$ $R_c = 132\Omega$ $E_c = 0.05\,V$

Fig. 13 Transient Response (Decaying)

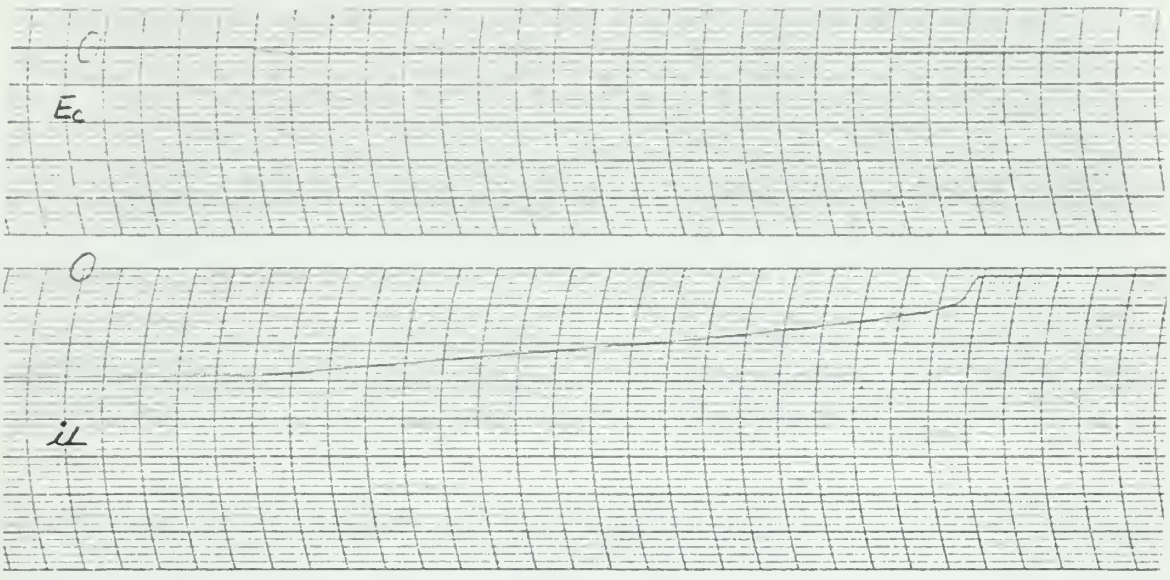

g) $E_S = 12V$ $R_L = 500\Omega$ $C = 0.6\mu f$ $R_c = 132\Omega$ $E_c = 0.035V$

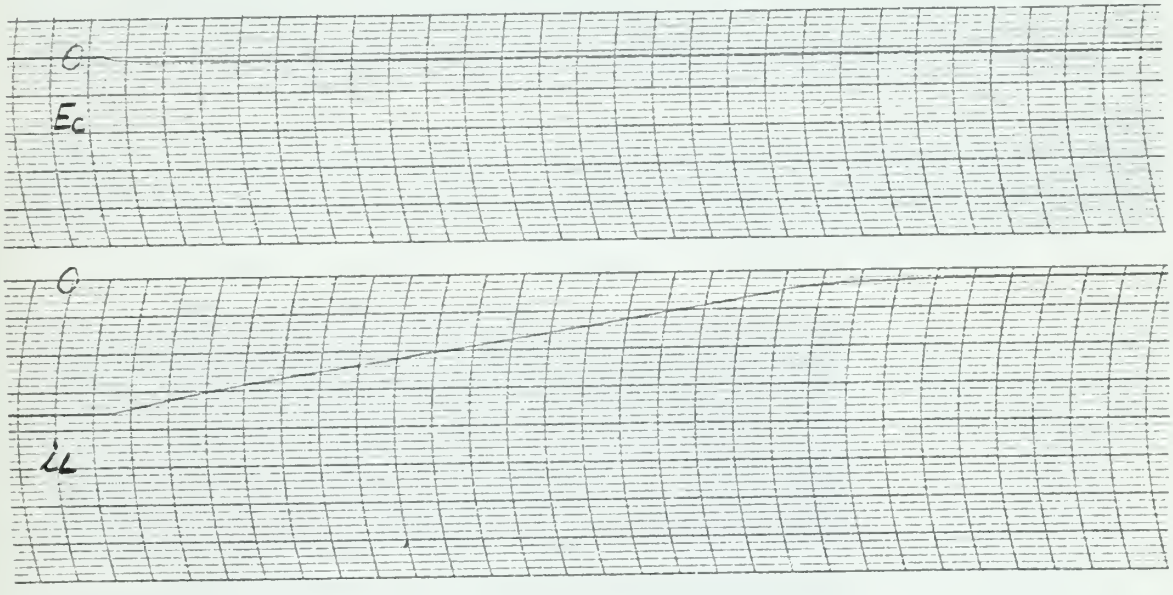

h) $E_S = 12V$ $R_L = 500\Omega$ $C = 1.0\mu f$ $R_c = 132\Omega$ $E_c = 0.035$

Fig. 13 Transient Response (Decaying)

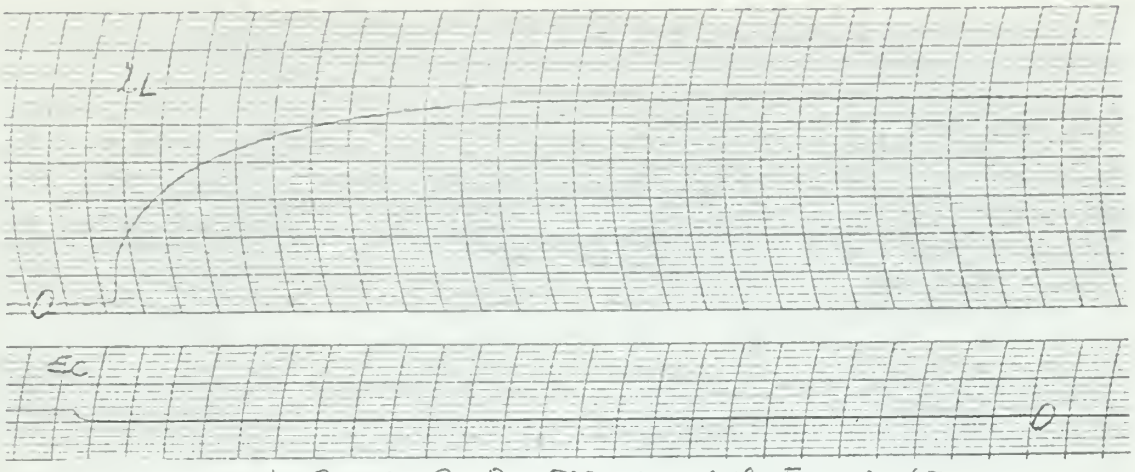

a) $E_s = 22\ V$ $R_c = 132\ \Omega$ $R_L = 500$ $C = 1.0\mu f$ $E_c = 0.065\ V$
delay time = 36 msec

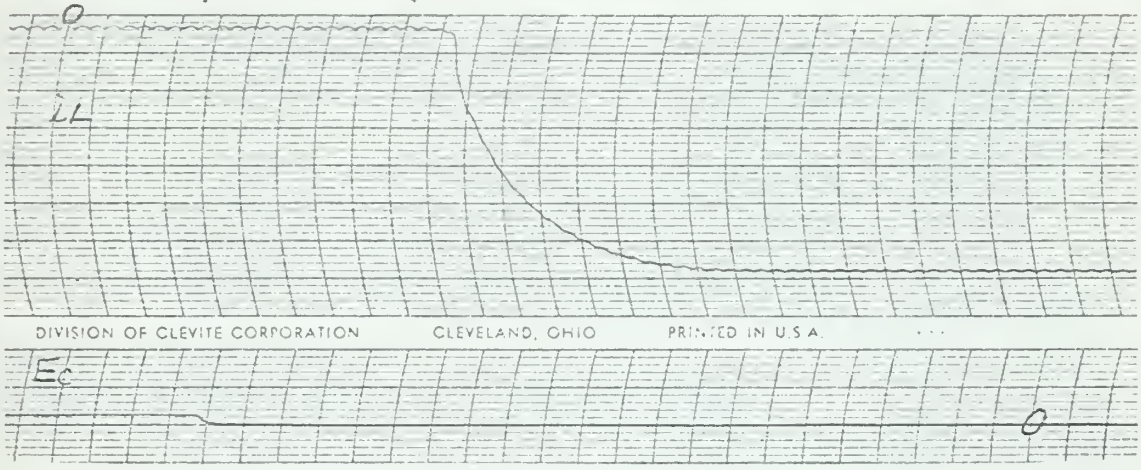

b) $E_s = 15V$ $R_c = 132\ \Omega$ $R_L = 500\ \Omega$ $C = 1.0\ \mu f$ $E_c = 0.05\ V$
delay time = 260 msec

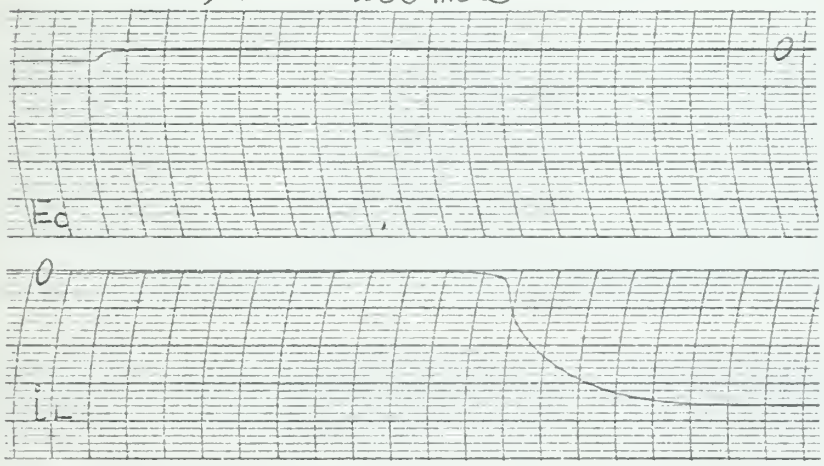

c)
$E_s = 12\ V$
$R_c = 132\ \Omega$
$R_L = 500\ \Omega$
$C = 1.0\mu f$
$E_c = 0.06\ V$
delay time
= 412 msec

Fig. 14 Long Delay before Rising.

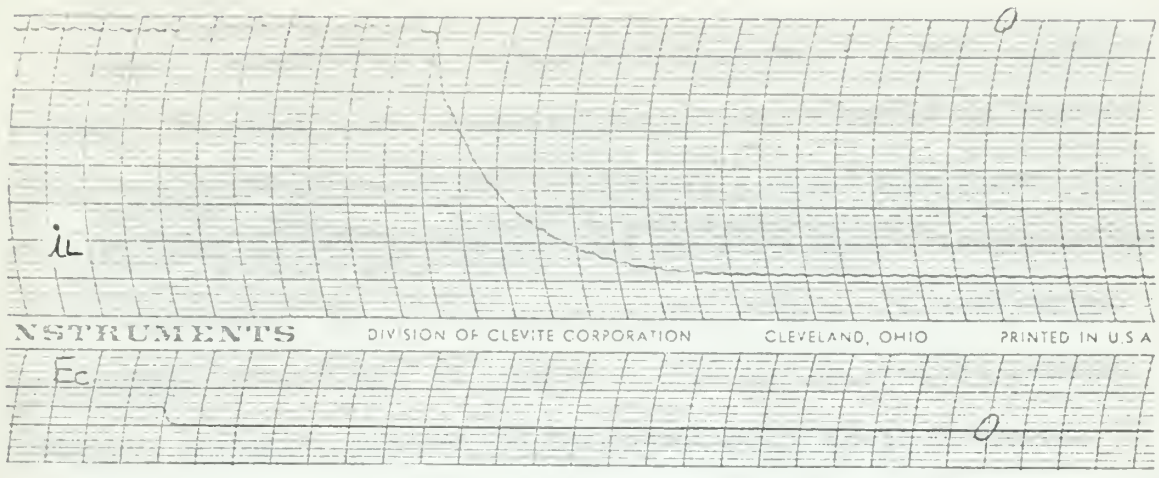

d) $C = 1.0\mu f$ $E_c = 0.1\ V$ delay time = 280 msec

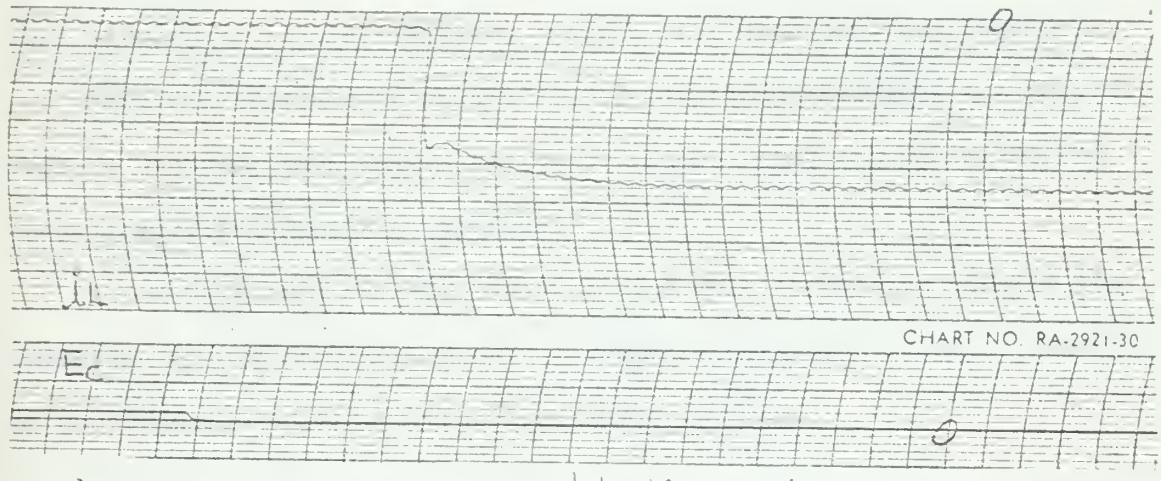

e) $C = 0.5\mu f$ $E_c = 0.05 V$ delay time = 240 msec

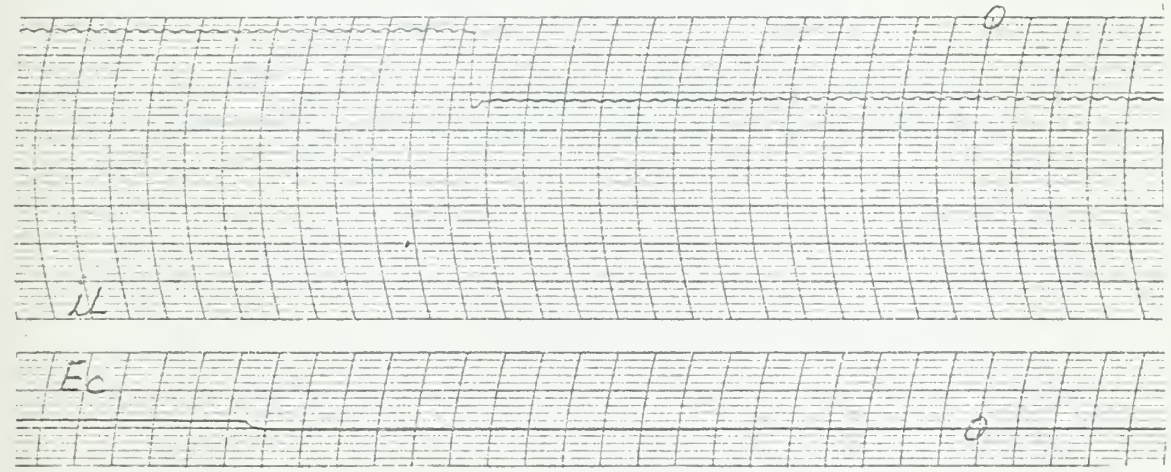

f) $C = 0.2\mu f$ $E_c = 0.05 V$ ($E_s = 15 V$ $R_c = 132\Omega$ $R_L = 500\Omega$ are Common)
delay time = 230 msec

Fig. 14. Long Delay before Rising

8. Conclusions

Magnetic Amplifiers have complicated characteristics with capacitive loading. The steady state characteristic transfer equation has been derived using difference equations and applying a square wave source voltage. The analytical results are compared with the experimental results and are in fair agreement. Due to the charge on the capacitor the term saturation voltage can no longer be applied in this circuit, and the maximum applicable voltage is derived and the normalized curve is presented.

Transient response is not solved analytically, but the effects of circuit parameters on the transient response are discussed qualitatively.

From the experiment, some of the interesting phenomena are observed such as jumping, long delay, and oscillation. They are discussed and correlated with circuit parameters.

It is felt that further investigation must be done to clarify the mechanism of the oscillation and to derive a transient transfer function of the magnetic amplifier with capacitive loading.

BIBLIOGRAPHY

1. H. C. Bourne, J. T. Salihi, Analysis of Series-Connected Saturable Reactor with Capacitive Loading and Finite Control Resistance by Difference Equations, AIEE Communication and Electronics, Vol 78 pp 461--471, Nov.,1959.

2. H. F. Storm, Magnetic Amplifier, John Wiley & Sons, Inc., 1955.

3. H. W. Collins, Capacitive Coupled Magnetic Amplifier, AIEE Communication and Electronics, Vol. 78, pp 707-712, Nov., 1959.

4. B. W. Lovell, Two-Step Switching of Saturable Reactors, AIEE Communication and Electronics Vol. 78 pp 895-900, Jan ., 1960.

5. H. H. Britten, Characteristics of Magnetic Amplifiers Utilizing Square-Loop Core Material and Square-Wave Supply Voltage, AIEE Communication and Electronics Vol. 77, pp 590-597, Nov., 1958.

6. P. R. Johannessen, Analysis of Magnetic Amplifiers by The Use of Difference Equations, AIEE Communication and Electronics, Vol 73, pp 700-711, Jan., 1955.

7. S. B. Batdorf, W. N. Johnson, An Instability of Self-Saturating Magnetic Amplifiers Using Rectangular Loop Core Materials, AIEE Communication and Electronics, Vol. 22, pp 223-227, July, 1953.

8. AIEE Committee Report, Recommended Symbols for Magnetic Amplifier Papers, AIEE Communication and Electronics Vol. 78, pp 519-520, Nov., 1959.